Atmos. Chem. Phys., 10, 10161–10185, 2010
www.atmos-chem-phys.net/10/10161/2010/
doi:10.5194/acp-10-10161-2010

Atmospheric Chemistry and Physics

New trajectory-driven aerosol and chemical process model Chemical and Aerosol Lagrangian Model (CALM)

P. Tunved[1], **D. G. Partridge**[1], **and H. Korhonen**[2]

[1]Department of Applied Environmental Science Stockholm University, 106 91, Stockholm, Sweden
[2]Finnish Meteorological Institute, Kuopio Unit, P.O. Box 1627, 70211 Kuopio, Finland

Received: 24 May 2010 – Published in Atmos. Chem. Phys. Discuss.: 21 June 2010
Revised: 28 September 2010 – Accepted: 28 September 2010 – Published: 1 November 2010

Abstract. A new Chemical and Aerosol Lagrangian Model (CALM) has been developed and tested. The model incorporates all central aerosol dynamical processes, from nucleation, condensation, coagulation and deposition to cloud formation and in-cloud processing. The model is tested and evaluated against observations performed at the SMEAR II station located at Hyytiälä (61°51′ N, 24°17′ E) over a time period of two years, 2000–2001. The model shows good agreement with measurements throughout most of the year, but fails in reproducing the aerosol properties during the winter season, resulting in poor agreement between model and measurements especially during December–January. Nevertheless, through the rest of the year both trends and magnitude of modal concentrations show good agreement with observation, as do the monthly average size distribution properties. The model is also shown to capture individual nucleation events to a certain degree. This indicates that nucleation largely is controlled by the availability of nucleating material (as prescribed by the $[H_2SO_4]$), availability of condensing material (in this model 15% of primary reactions of monoterpenes (MT) are assumed to produce low volatile species) and the properties of the size distribution (more specifically, the condensation sink). This is further demonstrated by the fact that the model captures the annual trend in nuclei mode concentration. The model is also used, alongside sensitivity tests, to examine which processes dominate the aerosol size distribution physical properties. It is shown, in agreement with previous studies, that nucleation governs the number concentration during transport from clean areas. It is also shown that primary number emissions almost exclusively govern the CN concentration when air from Central Europe is advected north over Scandinavia. We also show that biogenic emissions have a large influence on the amount of potential CCN observed over the boreal region, as shown by the agreement between observations and modeled results for the receptor SMEAR II, Hyytiälä, during the studied period.

Correspondence to: P. Tunved
(peter.tunved@itm.su.se)

1 Introduction

The representation of particles in the atmosphere remains one of the largest uncertainties in predicting our future climate (IPCC, 2007). Knowledge of the particle abundance, chemistry and size is of crucial importance to determine both indirect and direct climate effects of particles in the atmosphere. In order to accurately describe the aerosol properties on large spatial scales, more efficient ways to parameterize important aerosol processes are needed. While regional and global transport models incorporating aerosol schemes are quite numerous, they often include quite coarse parameterizations of the dynamical processes relating to aerosols in the atmosphere. Typically, this is due to computational limitations.

A more detailed description of aerosol processes is possible in coupled chemical-aerosol box models, which have been previously developed and tested in different environments. These models have been of varying level detail, and often used to address specific problems or questions in different types of environments (e.g. Capaldo, Kasibhatla and Pandis, 1999; Grini et al., 2005; Chameides and Stelson 1992; Danilin et al., 1994; Real et al., 2007). Box models are computationally efficient since they omit the advection term from the continuity equation, and simulate processing in a flow relative framework. This gives the opportunity to investigate the usually computationally demanding aerosol dynamic processes with a higher level of detail than possible in large scale regional or global models.

Published by Copernicus Publications on behalf of the European Geosciences Union.

In this study we present a new box model framework adopting state of the art aerosol dynamic description that will aid in the understanding of the different processes affecting the aerosol over the boreal regions, and in the future also at other sites. The model is a two layer box model that is intended to run along trajectories.

The aim with the study is to test this trajectory driven Lagrangian process model that seeks to capture and describe the processes that govern the evolution of aerosol chemical and physical properties. In this study we have focused on the processes dominating the aerosol as observed at Hyytiälä SMEAR station, Southern Finland (61° 51′ N, 24° 17′ E, 181 m a.s.l.). The SMEAR station has the longest record of aerosol number size distribution observations, dating back to 1996, and also facilitates numerous measurements of other aerosol parameters and trace gases. The surroundings are dominated by a flora mainly consisting of pine forests of an age of roughly forty years. The closest large city is the city of Tampere some 60 km away from the station. The location of Hyytiälä, in the southern rim of the Scandinavian boreal region, makes it an excellent site to study both the role of anthropogenic as well as natural emissions. The location allows studies of natural sources when the air masses originating from the marine environment transport over the forest, as well as of aged anthropogenic air downstream of the large pollution sources in continental Europe. This fact has been demonstrated in a number of studies, and northerly and southerly transport of air is associated with distinct features. As has been shown in previous studies, marine air transport over the forested regions is associated with a rapid increase in aerosol number and, to a somewhat smaller extent, in mass (e.g. Tunved et al., 2006a, b). This increase in number appears to be controlled by nucleation mediated by sulfuric acid while the growth mainly seems to be facilitated by organics originating from the forest itself, most likely monoterpenes (MT) or similar compounds (e.g., Tunved et al., 2006a; Laaksonen et al., 2008). However, when polluted air arrives from the south it is seen that nucleation is largely absent over the forest, and number concentrations typically decrease when transport further northwards takes place (Tunved et al., 2005). Although located far from major pollution sources, observations at Hyytiälä do show that continental influence may occasionally dominate the aerosol properties (Dal Maso et al., 2007; Tunved et al., 2003) providing the site with a fairly large concentration of accumulation mode-sized particles.

In this study we use the newly developed model CALM to study the integrated effect of both natural and anthropogenic sources, as well as primary and secondary aerosol production. Using a number of sensitivity tests, we identify the processes dominating the appearance and abundance of particles associated with air-masses of different origin. The difference between e.g. marine and continental air sources will be discussed in terms of the role of primary and secondary emissions. Several other model studies have been performed at Hyytiälä, covering a wide range of complexity (Eulerian process studies, Lagrangian process studies, Tunved et al., 2004, global model studies, Spracklen et al., 2006). Aside from the general features of the aerosol, many of these studies have focused on the role and mechanisms of nucleation over the forest and on the importance of primary emissions.

2 General model design

The basic model design consists of a trajectory driven box model. The model is fed with back trajectories along which the process model simulates the evolution of both aerosol and gas species. The current model setup adopts a two layer structure, a residual and mixing layer (RL and ML, respectively). Both compartments are assumed to be well mixed internally. The trajectory dictates the transport of the model space described by these internally well mixed boxes. The trajectory itself however is not assigned specifically to either of the boxes, but instead describes the movement of this simplified model system along the geographical coordinates of the trajectory. Exchange between the layers is allowed, and this exchange is governed by the variation of the mixing layer height (MLH). The MLH typically follows a diurnal cycle with a maximum around noon. The MLH is calculated by the HYSPLIT4 model along the trajectories and is defined as the height level at which the potential temperature is at least two degrees greater than the minimum potential temperature. During morning hours, when the mixing layer starts to grow into the residual layer, the mixing layer gases and aerosols are mixed with their counterparts in the residual layer, a process that most of the time leads to dilution of the ML quantities. When the MLH starts to decrease, the ML aerosol and gases get partially trapped within the residual layer. The height of the mixing layer is provided by the trajectory model and typically varies between 250 m (which is the lower limit from the trajectory model) and some thousand meters above the ground level. Throughout each simulation the residual layer upper limit remains constant. This upper boundary of the model compartment is defined as the maximum MLH of each simulated trajectory and typically reaches altitudes around 1500–2500 m. There are no interactions with the air above the modeled layers in the current set-up.

The trajectories were calculated using the HYSPLIT4 model on FNL data. The FNL data is a product of the Global Data Assimilation System (GDAS), which uses the Global spectral Medium Range Forecast model (MRF) to assimilate multiple sources of measured data and forecast meteorology (Draxler and Hess, 1998). Trajectories were calculated arriving 100 m above ground level (m a.g.l.) Along each trajectory, surface temperature and surface wind speed were extracted from the meteorological data fields. This data is needed for the approximation of temperature dependent BVOC emissions and of wind speed dependent

emissions from water surfaces. Other relevant meteorological parameters, such as relative humidity and ML height, were extracted from trajectory calculations as well.

In both layers we allow for general aerosol dynamics (e.g. condensation, nucleation, coagulation) as well as photochemistry. However, deposition is only considered in the ML and all ground based emissions are initially confined to the ML, although may be transported into the RL due to variation of the MLH. Two types of clouds are considered: stratus type and cumulus type clouds. The model setup only allows for clouds in the mixing layer. The frequency of clouds is described using available statistics of cloudiness over the model domain. Precipitation scavenging is accounted for in both ML and RL. The treatment of these processes will be described in detail below.

2.1 Aerosol dynamic model

The aerosol particle dynamics is described using the University of Helsinki Multicomponent Aerosol model (UHMA) described in detail by (Korhonen, Lehtinen and Kulmala, 2004). The model incorporates the major microphysical processes that affect the aerosol under clear sky conditions, namely nucleation, coagulation, multi-component condensation and dry deposition. In the current model setup we assume that the aerosol is distributed over 45 log-normally distributed bins over the size range 0.2 nm–1.2 µm. The particles are assumed internally mixed in every size bin. In each bin we allow a composition defined by three different components: sulfuric acid, soluble organics and insoluble species. In the setup we assume that component one represents sulfur and sea salt, component two represents both primary and secondary formed organic aerosol constituents and component three represents insoluble species (i.e. soot in the current setup).

Nucleation is represented by the activation theory, where the nucleation rate is directly proportional to the concentration of sulfuric acid, [H_2SO_4], with an empirically defined correlation coefficient, A (Kulmala, Lehtinen and Laaksonen 2006). The value of A has been set to 2×10^{-6} following empirical findings at Hyytiälä (Riipinen et al., 2007). It is worth mentioning that A varies between different locations and seasons, reflecting the other unknown components necessary to accurately describe the rate of nucleation. Thus A may be described as an environment-specific constant, but since the information available on the value of A is still somewhat limited we assume that A remains constant through the simulations. As we will see, this will not substantially affect the final simulated size distribution at the receptor location.

The dry deposition for particles and gases is calculated for the 17 classes of land cover in the International Geosphere-Biosphere Programme (IGBP; Loveland and Belward, 1997) global vegetation classification scheme. The Land Cover Classification product (MOD12Q1) includes 11 natural vegetation classes, 3 developed land classes (one of which is a mosaic with natural vegetation), permanent snow or ice, barren or sparsely vegetated land, and water.

Dry deposition is calculated following the dry deposition procedure by the EMEP/MSC-E regional model of heavy metals airborne pollution (MSCE-HM), using variations on the resistance analogy approach (Wesely et al., 1989) for each surface type (as documented by Travnikov and Ilyin, 2005).

The dry deposition of gases is calculated following the gaseous deposition model by Zhang et al. (2003). This model utilizes a "big-leaf" resistance approach model for representing the process of gaseous deposition. It is very important to describe in some manner the deposition of terpenes within CALM. It is difficult to assign the gas properties, e.g. molecular diffusivities, for these organic compounds since there are very few measurements in the literature. Therefore for consistency the carbonyl groups presented by Zhang et al., 2003 are used as a proxy for these gases in CALM.

2.2 Chemical model

The gas-phase chemistry is solved using the quasi-stationary state assumption (QSSA). The chemistry module solves the chemistry for every time step of the simulation, thereby updating the concentration of the included species. Besides chemical reactions, the trace constituents are also subject to deposition (wet and dry) and removal from the gas phase via condensation onto existing particles (and naturally also nucleation, as in the case for sulfuric acid, see Sect. 2.2). In this study we estimate the chemistry for 76 different compounds and intermediates. The module solves the chemistry of the most important oxidants; hydroxyl radicals (OH, HO_2), nitrate radicals (NO_3) and ozone (O_3).

In the model, the photolysis constants are taken from a lookup table were the constants have been calculated using the Tropospheric Ultraviolet-Visible Model (TUV, Madronich et al., 2002) under different atmospheric conditions. Additional modules to process the lookup table is also used (JVAL1, Madronich et al., 2002). The photolysis constants for 56 different reactions are extracted from the look-up table. The selection is based on solar zenith angle, azimuth and atmospheric properties such as optical depth and concentration of absorbing gases. The solar zenith angle and azimuth constants are computed from the geographical information supplied by the HYSPLIT4 output, i.e. latitude, longitude, time and date. In our set up we have fixed the optical depth to 0.1 and the single scattering albedo to 0.85. Most likely, these values will vary significantly over the modeled domain. However, we do not have the possibility to specifically address these properties more in detail. The ozone column aloft is assumed to be 330 Dobson units. The surface albedo is set to 0.3 throughout the simulations. If clouds are present in the model run, TUV photolysis

constants are adjusted accordingly, assuming a cloud optical depth of 20 (corresponding to reasonable cloudiness), modifying photolysis constants above (i.e. in the residual layer) and below the cloud column (i.e. in the mixing layer).

The terpene chemistry is represented by the relatively well-known reaction chain of α-pinene, and the reaction scheme used is the one presented in (Andersson-Skold and Simpson 2001)and references therein. This reaction scheme includes the reactions of α-pinene and its products considering oxidative reactions including nitrate radicals (NO_3), hydroxyl radicals (OH) and ozone (O_3). While the reactions described in this scheme certainly are important for the gas phase chemistry, e.g. radical abundance and ozone production, we do not use the products in this scheme explicitly when estimating the production of condensable species. Instead, we assume a fixed stochiometric yield of 15% condensable compounds from the primary reactions between α-pinene and NO_3, OH and O_3. This compound is assumed to have saturation vapor pressure of 3×10^{12} molecules per cubic meter, and molar mass of 186 g mol^{-1} (Kulmala, Laaksonen and Pirjola, 1998). The yield agrees well with earlier estimates presented by Tunved et al. (2006b) (using 13%) considering what is required to reproduce the observed growth rates of particles over the boreal forest.

Isoprene chemistry follows the scheme suggested by Simpson et al. (EMEP, MSC-W, 1993), including 18 different reactions of isoprene and its products.

Sesquiterpenes are assumed to be immediately oxidized once emitted, and thus we do not describe their chemistry at all. Sesquiterpenes are highly reactive, and are quickly oxidized under atmospheric conditions. Chamber studies indicate that the aerosol mass yield from its oxidation by common oxidants is between 17–67% (Griffin et al., 1999). In our setup 20% of the emitted sesquiterpenes are assumed to form a condensable product with the same properties as that formed from mono-terpene oxidation.

In the current setup, ethane is assumed to represent all anthropogenic NMVOC emissions. The chemistry of ethane is described using the reaction sequence presented by Simpson et al. (EMEP, MSC-W, 1993). The same goes for the methane chemistry.

With the reactions outlined above, the chemistry of NO_x is solved and the ozone HO_x (OH, HO_2) and nitrate radical concentrations are calculated.

2.3 Cloud description

The occurrence of clouds is prescribed randomly in the model. The cloud frequency, however, is constrained by observational seasonal data. The cloud frequency for different seasons and locations (Dec–Feb, Mar–May, Jun–Aug, Sep–Nov) are adopted from the online Climatic Atlas of Clouds over Land and Ocean (http://www.atmos.washington.edu/~ignatius/CloudMap/, Warren et al., 2006). This approach allows for both seasonal and spatial constraints with respect to cloud frequency over the simulated domain. The cloud types considered are stratus type clouds and cumulus type clouds. The stratus type clouds fill the upper 150 m of the ML. The typical coverage of the stratus clouds is set to 6/8. The cumulus type clouds are assumed to form from the middle of the mixing layer up to the top of the mixing layer. Furthermore cumulus clouds are only present when the mixing layer height is above 600 m. The typical coverage of the cumulus type clouds is set to 4/8 or 50%. This means that only a fraction of the aerosol will be processed by a cloud, and this fraction is based on the horizontal coverage and vertical extent of the cloud as described above.

When a cloud is assumed to form, the ML aerosol size distribution and associated properties are fed to the cloud module, where the dynamics of the aerosol population in the clouds is described using the common growth equations (e.g. Seinfeld and Pandis, 1998), using a constant updraft through the cloud. The updraft in turn depends on the cloud type. Stratus type clouds are allowed to have a prescribed updraft between 0.025–0.125 ms^{-1} and the cumulus type clouds are allowed to have an updraft between 1–3 ms^{-1}. Although fixed for the individual clouds simulated, the updraft for every cloud cycle is determined randomly, allowing the updraft to vary within the above-mentioned limits from case to case. The growth is calculated based on the size and composition of the aerosol particles. Sulfates are assumed to be completely soluble, while the solubility of the organics is assumed to be 10%. Variable aerosol properties (such as size and chemistry) and variable updraft will thus govern a variation in lowest activation radius from case to case. The droplet growth in the cloud is described using the moving center approach, in contrast to the fixed sectional approach adopted for the "dry" aerosol dynamics.

Once a cloud is formed, cloudy conditions are assumed to apply for 4 h. However, since clouds are dynamic , their physical properties and environmental parameters change through time. This means that a static cloud with constant properties during four hours would be unrealistic. We bypass this issue by allowing the cloud properties (base-height, thickness (as for cumulus clouds), LWC and droplet distribution) to remain constant for only 15 min. After 15 min the cloud dissipates and the cloud-processed aerosol is mixed with the rest of the mixing layer aerosol before it is recalculated from an updated aerosol size distribution and updraft. In this way, for every cloud period, the cloud is recalculated 16 times. This 15 min cycle is applied in order to prevent an unrealistic behavior of the cloud, and allows the cloud to be replenished with gases and aerosol, thereby trying to imitate the actual dynamics of clouds. Due to the overall simplicity of the model structure, we do not think that we are able to describe convective clouds in a detailed way. Thus we do not consider convective clouds or associated precipitation events in the model.

The current setup of clouds allows for no precipitation, and thus no in-cloud scavenging. This is admittedly a compromise. Several attempts were made to mimic the in-cloud scavenging by allowing the shallow clouds to precipitate. However, the results soon became unrealistic since the aerosol was removed too quickly from the modeled two layer column. Thus, it was concluded that the current setup could not provide realistic precipitation description. Instead, precipitation data ($mm\,h^{-1}$) are taken from the HYSPLIT4 model output. This precipitation is assumed to fall through both the RL and ML, but the precipitating cloud itself is formed above the modeled column. In practice, this means that explicit treatment of in-cloud scavenging is omitted in the model since the cloud is formed on an aerosol outside the modeled column. This approach is likely valid for frontal type precipitation (i.e. nimbostratus) considering that (1) the front itself serves as a boundary between two air-masses and (2) the air flows behind and ahead of the front are not the same since they occur in different air-masses. In practice, the movement of a warm front includes lifting of the warm air on top of the colder air-mass. Since the trajectories are calculated arriving at 100 m and given the fact that the trajectories rather seldom subside close to the station, the likelihood for a trajectory having spent time inside a NB-type cloud during the last couple of days is typically small. This means that rainout processes (i.e. in-cloud scavenging) are less likely to affect the mixing layer aerosol as compared to washout processes (i.e. below cloud scavenging) considering timescales of a couple of days. Thus, in the model we assume washout (i.e. below cloud scavenging) of aerosols only. For this purpose we make use of the parameterization presented by (Laakso et al., 2003). This empirically derived parameterization is based on 6 years of ground level size distribution data measured at Hyytiälä (61°51′ N, 24°17′ E) and provides size dependent scavenging coefficients between 10–500 nm. In this study, the parameterization is extrapolated up to 1 µm. Since the approach of the study presented by Laakso et al., incorporates size distribution data and precipitation data measured on the ground level, the resulting parameterization will largely describe below cloud scavenging, but since the approach relies on the measured rate of change in aerosol concentration versus precipitation intensity, also other processes will by necessity affect the rate of change in aerosol properties (i.e. size dependent number concentration). This means that the parameterization will also indirectly take into account in-cloud scavenging if the precipitation takes place in a cloud confined within a well mixed boundary layer.

The CALM cloud module further takes into account in-cloud oxidation of sulfate by ozone and hydrogen peroxide. We here use a bulk-water approach by summing up the total volume of water in the cloud. The bulk-water of the cloud is assumed to be infinitely dilute and is iteratively equilibrated to the surrounding gases (NH_3, SO_2, H_2O_2, O_3, CO_2) and pH is evaluated based on the amount of dissolved gases and aerosol bulk composition (considering the sulfate fraction only). The soluble gases (SO_2, NH_3, O_3 and H_2O_2) are partitioned between gas and liquid phase based on thermodynamical limitations. The in-cloud oxidation of S(IV) to S(VI) is initialised by calculating the pH of the cloud bulk water, taking into account the liquid water content (LWC), concentration of surrounding gases and the particle content of sulfate. Once the pH has been established and the equilibrium of reacting gases has been reached, the liquid phase oxidation is calculated. The pH and concentration of reacting gases in the liquid phase are recalculated every time step.

$$d[\mathrm{S(IV)}_{\mathrm{O3}}]/dt = [\mathrm{O_3,aq}](k_0[\mathrm{H_2SO_3}] + k_1[\mathrm{HSO_3}^-] + k_2[\mathrm{SO_3}^{2-}]) \quad \text{(R1)}$$

$$d[\mathrm{S(IV)}_{\mathrm{H2O2}}]/dt = k_4[\mathrm{H_3O^+}][\mathrm{HSO_3^-}][\mathrm{H_2O_2,aq}]/(1 + K[\mathrm{H_3O^+}]) \quad \text{(R2)}$$

Reaction constants used are those from Seinfeld and Pandis (1998). When the cloud dissipates, the produced sulfate (equivalent amount of sulfuric acid) is distributed over the size range of activated particles following the sectional method. Each particle gains sulfate proportional to the individual water content of the droplet. This causes activated particles to leave the cloud with a larger size than they entered the cloud, and clouds thus provide a source of sulfate in the model.

The gas phase chemistry if further indirectly affected by cloudiness. When clouds are present, the photolysis constants are adjusted accordingly, assuming a cloud optical depth of 20 (corresponding to reasonable cloudiness), modifying photolysis constants above (i.e. in the residual layer) and below the cloud column (i.e. in the mixing layer).

2.4 Emissions

2.4.1 BVOC

In the model setup we consider biogenic emissions from different land use types according to the IGBP land use maps (Loveland and Belward 1997): needle leaf forest, mixed forest, deciduous needle leaf forest, open shrubs, closed shrubs, grasslands, permanent wetlands and croplands. The land use type is defined as a fraction per grid of the land use map (0–1 on a quarter degree grid). To apply a seasonal dependence on the foliar biomass density we adopt the Global Inventory Modeling and Mapping Studies (GIMMS) Normalized Difference Vegetation Index (NDVI, Tucker et al., 2004), from which we derive a foliar biomass density using the equations as presented in (Guenther et al., 1995)and references therein. The NDVI data is used as follows:

The monthly average of the Global vegetative indices (G) is calculated as:

$$G = 100(1 + \mathrm{NDVI}) \quad (1)$$

And the foliar biomass D_m density is calculated as:

$$D_m = D_p(\exp(\ln(2)((G - G_2)/(G_{\max} - G_2))) \quad (2)$$

D_p represents annual peak foliar density. D_m is only calculated if G is above a certain threshold $G2$. Representative values of G_2 are taken from (Guenther et al., 1995). Otherwise, D_m is set to zero. D_p is in turn calculated as

$$D_p = D_r \times \mathrm{NPP} \quad (3)$$

Where D_r is an empirical coefficient and NPP represent the net primary production taken from tabulated values for different ecosystem types corresponding to our IGBP land use classification.

The emission potential for spruce and pine is allowed to vary depending on season (Tarvainen et al., 2007). For deciduous forests we assume an emission potential of monoterpenes of µg g (dry weight)$^{-1}$ h^{-1} (i.e. emissions per hour and gram of leaf dry weight).

Biogenic Volatile Organic Compounds (BVOC) are assumed to consist of monoterpenes (represented by α-pinene), isoprene and sesquiterpenes. Concerning the mono- and sesquiterpenes emissions we assume pool dependent temperature controlled emissions (Guenther et al., 1993, 1995). Monoterpene emissions are strongly dependent on temperature and the total flux of terpenes can be calculated using the relation $F = \varepsilon D \gamma$, where F represent the total flux of monoterpenes from the forest in µg m^{-2} h^{-1}, ε is the emission potential (µg g (dry weight)$^{-1}$ h^{-1}), D is the foliar biomass density in g (dry weight) m^{-2}, and γ is an environmental correction taking into account the temperature dependency of the emission rate ($\gamma(\mathrm{pool}) = \exp(\beta\ (T - T_s))$, $\beta = 0.09\,\mathrm{C}^{-1}$ and $T_s = 303.15$).The temperature used is the surface temperature as derived from the FNL data set used for trajectory calculations. The sesquiterpenes are calculated in a similar manner, but with a seasonal dependence of the emission potential associated with conifer trees with a zero emission potential through November-March (Hakola et al., 2006). No light dependence is considered for monoterpene emissions. Isoprene is calculated following Guenther et al. (1995). This isoprene emission estimates adopts both light and temperature dependence. The photosynthetic photon flux density (PPFD) is calculated following (Alados-Arboledas et al., 2000). The clear sky values of the PPFD are used regardless of cloudiness in the model. The emission potentials used are 0.1 µg g (dry weight)$^{-1}$ h^{-1} for conifers and 1 µg g(dry weight)$^{-1}$ h^{-1} for deciduous trees.

2.4.2 Other trace gases

In its current form, the model allows for gridded emissions of the most common inorganic trace gases as well as anthropogenic emissions of non-methane volatile organic compounds (NMVOC). These emissions are taken from the EMEP data base (50×50 km grid, Vestreng et al., 2006) and include besides NMVOC (in our study represented by ethane) also CO, anthropogenic SO_2, natural SO_2, and NO. The emissions are adjusted to comply with the seasonal emission pattern (D. Simpson, personal communication, 2007). DMS emissions are calculated according to (Kettle et al., 1999), making use of monthly mean sea surface DMS concentrations. Actual DMS fluxes are calculated from these surface water concentrations by using surface temperature and wind speed.

2.4.3 Primary emissions

The model also incorporates primary aerosol emissions. For this purpose, the model includes anthropogenic emissions of anthropogenic primary organic particles (POA) as well as POA emissions from forest fires. These emissions are taken from the AEROCOM database (Dentener et al., 2006)using year 2000 as reference. The emissions are mass based, but remapped to standard size distributions as shown in Table 1. The seasonal dependence for the emissions is accounted for by applying the previously discussed seasonal scaling factors also for these data sets. The forest fire emissions are however given as monthly values throughout the year. Sea spray emissions are estimated assuming dependence on wind speed and temperature following (Martensson et al., 2003).

3 Results

In the following the general model performance will be discussed followed by an investigation of the model's sensitivity to certain key processes/parameters. The model is initialized with either a marine, rural or polluted continental size distribution, depending on the starting location. The model parameters of these initial size distributions are given in Table 2. The model is further initialized, regardless of starting location and/or time of year with 35 ppb ozone, 40 ppt SO_2 and 500 ppt NO_x. CO is a rather long lived species and also plays an important role in regulating the abundance of oxidants in the atmosphere. Therefore, initial CO concentrations are selected based on both season and location, i.e. either summer or winter values for continental and marine starting locations (100 and 220 ppb for summer and winter time continental locations and 100 and 150 ppb for summer and winter marine locations, thereby adopting typical values to initialize the model). All BVOC are initially set to zero. Methane is set to 1750 ppb.

3.1 A single trajectory run: simplified description of processes

In order to show the evolution of some selected key parameters along a trajectory run we selected a case where marine air is advected over Scandinavia (Fig. 1). Time and date of this simulation ends at 13 April 2000, 06:00 UTC. The model was simulated along the trajectory shown in Fig. 1 for 216 h, i.e. 9 days, starting in the marine Arctic environment. The evolution of selected parameters is displayed in Fig. 2, where the concentration of SO_2, O_3, H_2SO_4, (condensable organics), mixing layer height and cloudiness are shown. This plot

Table 1. Adopted size distribution properties of the various AEROCOM primary emissions. Shown is the sigma and geometric mean for the emission size distribution and emission year used for each sector.

Parameter	D_g	Sigma (σ_g)	Year	Reference
Biofuel Soot	80 nm	1.8	2000	Bond and Streets, 1996
Biofuel POM	80 nm	1.8	2000	Bond and Streets, 1996
Fossil fuel Soot	30 nm	1.8	2000	Bond and Streets, 1996
Fossil fuel POM	30 nm	1.8	2000	Bond and Streets, 1996
Forest Fires Soot	80 nm	1.8	2000	Global Fire Emissions Database (GFED) version 1[a]
Forest fires POM	80 nm	1.8	2000	Global Fire Emissions Database (GFED) version 1[a]

[a] http://ess1.ess.uci.edu/~jranders/data/GFED2/

is accompanied by Fig. 3 showing the evolution of aerosol number size distribution along the trajectory (top frame) as well as the observed evolution of the aerosol number size distribution as observed at Hyytiälä during the final day of the simulation (lower frame). As can be seen from the figures, as long as the air resides over the marine environment, some nucleation is taking place, but the magnitude of both nucleation and growth is too low to support production of particles that will be stable for a longer period of time. However, as soon as the air arrives at the coast, the onset of biogenic emissions (represented by MT, third panel in Fig. 2) provides the amount of organic gases to support the growth. The air parcel reaches the coast after approximately 144 h of simulation, and during the following days, three consecutive nucleation events are suggested by the model, of which each one is contributing to increasing number concentration. The simulated day is also associated with nucleation at the receptor site Hyytiälä which is evident from Fig. 3 (lower frame), a typical feature observed at this station when marine polar and arctic air masses arrive at the station. The idea that the forest supports the growth has been pointed out in numerous studies as discussed in the introduction and the current model result suggests that several consecutive, nucleation events provide the number concentration that is observed at the station when this type of transport takes place. As a comparison, the resulting simulated and observed aerosol number and volume size distributions are shown in Fig. 4. Although the growth is slightly smaller of the simulated distribution, there is a good agreement between the modeled and measured distributions. The total volume is further larger for the modeled data compared to the observed data as evident from second frame of Fig. 4. This also causes increased condensation sink, which may be part of the explanation of the slower growth of the

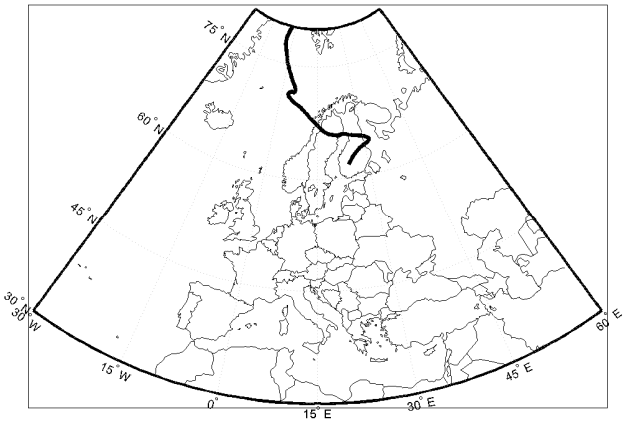

Fig. 1. Trajectory arriving Hyytiälä at 13 April 2001 06:00 UTC.

modeled nuclei mode. It should however be mentioned that while the agreement in this specific case is comparably good, some of the other simulations result in size distributions that on short time scales are quite different from the observations. The sometimes poor agreement may be due to wrong description of cloudiness, inaccurate transport paths of simulated boxes or wrong representation of sources to mention a few possible causes.

The influence of clouds is also displayed in the figures: as can be seen in the bottom panel of Fig. 2 five cloud events are prescribed by the model. The role of clouds becomes clear by comparing the onset of cloudiness after around 150h of simulation. When the cloud forms at this time of simulation, the sulfur dioxide concentration is sufficiently high to provide an important source of particle sulfate via in cloud production. This is evident looking at the corresponding time

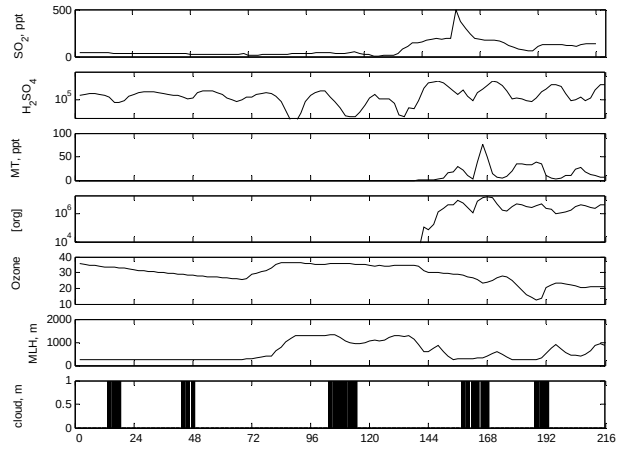

Fig. 2. Evolution of trace gases and meteorological parameters during the 216 h simulation along the trajectory shown in Fig. 1. Sulfuric acid and condensable organic species are in units of molecules cm^{-3}. Ozone and SO_2 in ppb's and ppt's, respectively. Clouds are shown as either on or off, giving values of 1 or 0, respectively.

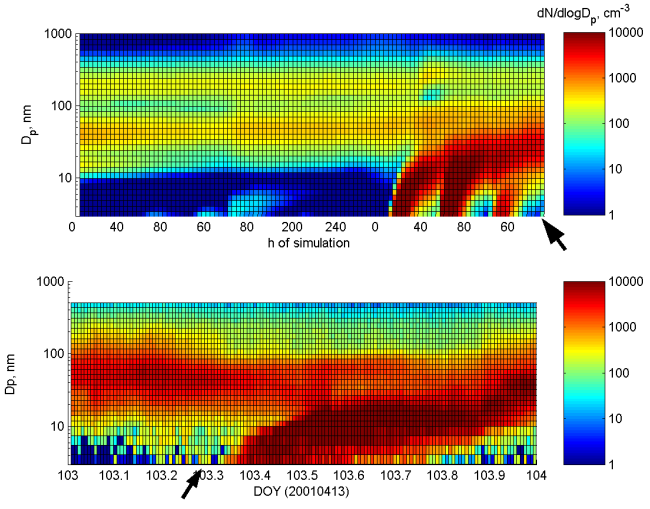

Fig. 3. Evolution of the mixing layer aerosol number size distribution along the trajectory ending in Hyytiälä 13 April 2001 06:00 UT (top frame) and the evolution of the aerosol number distribution during the final day of simulation as observed at the SMEAR II station in Hyytiälä (lower frame). The arrows denote where the simulated and observed data are compared in following Fig. 4.

in Fig. 3. The population of activated CCN's evaporates and leaves behind significantly larger particles than those entering the cloud. This is clearly shown by the evolution of the minimum developing around 110 nm concurrent with the onset of cloudiness, shifting these particles into a larger size range.

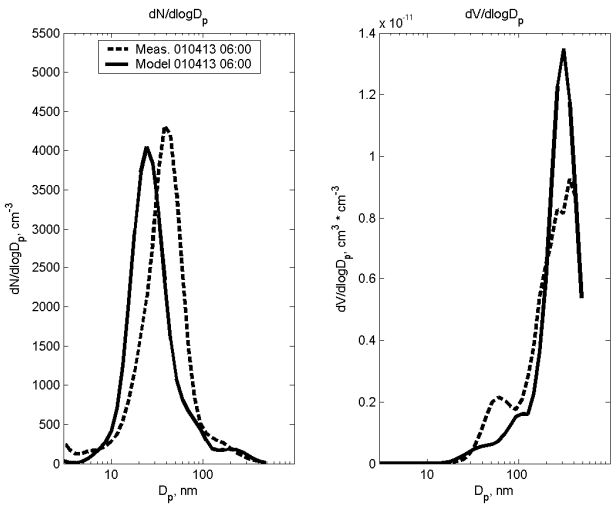

Fig. 4. Comparison between modeled and measured number (left) and volume (right) size distribution as of 13 April 2001, 06:00 UTC. Mixing layer, Hyytiälä.

3.2 Comparison with observational data

Both aerosol properties and trace gases will be discussed under two separate paragraphs under this section. As a base case reference years we have chosen years 2000–2001. For this period, 4 trajectories have been calculated each day (00, 06, 12 and 18). The model has been run along these trajectories, thus supplying the following model-measurement comparison with four endpoints each day throughout the two years. This provides the necessary model output required to perform both seasonal and monthly averaging of the data. This modeling approach also allows for Eulerian interpretation of the simulated data and thus straightforward comparison with observations.

3.2.1 Aerosol properties

In the following we show the results from the modeled and measured aerosol physical properties. In order to allow a direct comparison between the measured and modeled results, the modeled data was remapped to the bin width and size of the measured data using Matlab Spline fitting. This gives the measured and modeled data identical structure, while still introducing a minimum of bias to the data.

Shown in Figs. 5 and 6 are the comparisons between measured and observed aerosol number size distributions for years 2000 and 2001, respectively. The figures display the monthly average measured size distributions and their corresponding 25-th–75-th percentile range. The modeled data is shown by the thick black line. The model is capable of reproducing the typical features of the observational data, as monthly average, with a relatively good accuracy for 9 of 12 months for year 2000. The modeled data typically falls

Table 2. Number of trajectories belonging to each one of the clusters

Source region	N1	GSD1	Dg1	N2	GSD2	Dg2	N3	GSD3	Dg3
Marine	60	1.19	14	235	1.43	37	110	1.44	170
Rural	6650	1.252	15	147	1.745	54	1990	1.305	84
Remote continental	111	1.52	35.6	326	1.45	67.6	204	1.6	167

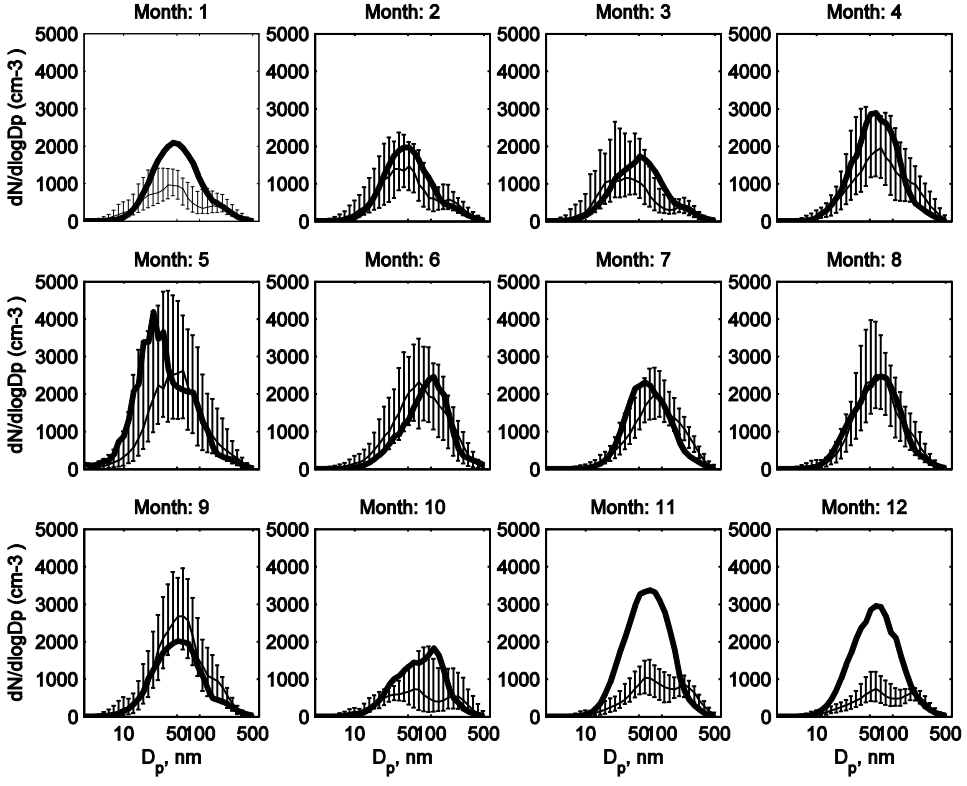

Fig. 5. Monthly median modeled size distributions (thick black line) and 25-th–75-th percentile (thin black line + errorbars) for correspionding observational aerosol number size distribution data, Hyytiälä, 2000.

within the modeled 25-th–75-th percentiles of the measured results, and occasionally the modeled monthly median agrees very well with observed values (e.g. February, September, July and August). Not only the overall magnitude of the measured data is captured by the model during these months but also the shape of the size distribution is properly represented, and follows the changes in observational data, i.e. towards mono- or bimodal structure. Also for year 2001 model and measurements show a good agreement, apart from January-December. This indicates that the model in general is capable of reproducing the influence from relevant processes and sources. It is however obvious that the model performs worst during the winter months, especially December and January.

Table 3. Modal parameters of the input size distributions. N(1–3) corresponds to number of particles in each mode (cm^{-3}), GSD(1–3) correspond to the geometric standard deviation of each mode, and Dg(1–3) represents modal size in nm.

Cluster number	1	2	3	4	5	6	7	8	9	10
# trajectories	94	132	58	207	144	140	89	71	63	97

In these cases the model overestimates the observational data and further suggests a typically uni-modal size distribution, while the measured size distribution is bi-modal.

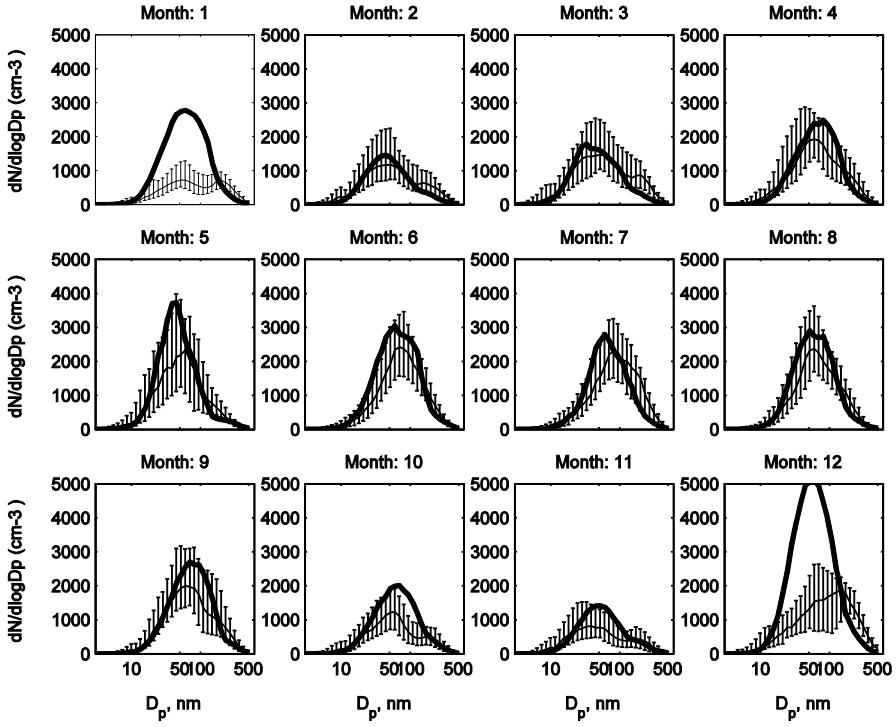

Fig. 6. Monthly median modeled size distributions (thick black line) and 25-th–75-th percentile (thin black line + errorbars) for correspiond-ing observational aerosol number size distribution data, Hyytiälä, 2001.

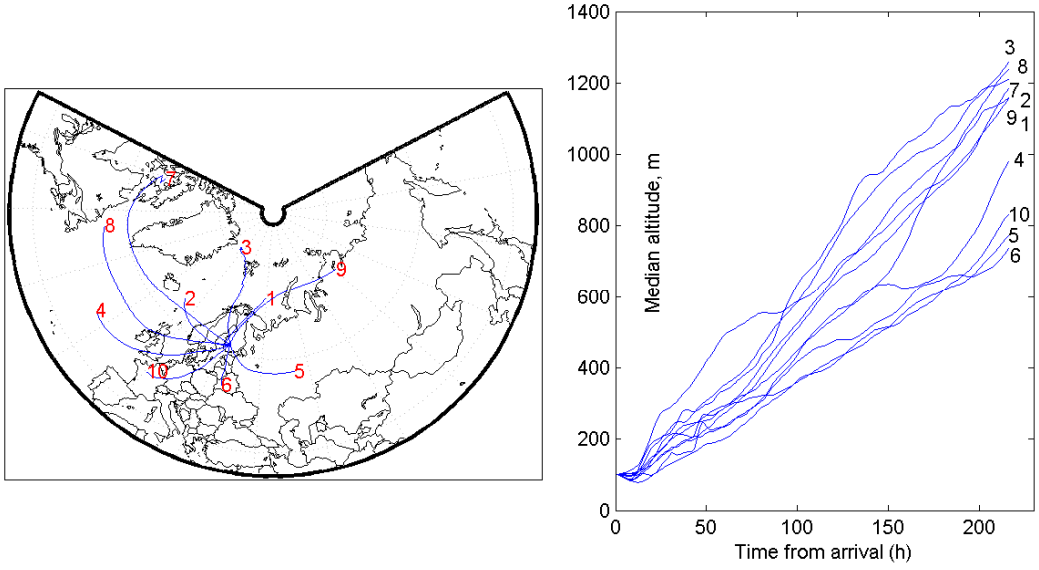

Fig. 7. The ten trajectory clusters resulting from the clustering. Cluster number is indicated at the end of each centroid (left frame). Right frame shows the median altitude along the clusters.

It may also be informative to study how the model performs when the air arrives from different source regions, since such an analysis could aid in finding areas where sources and/or processes are less well captured. Therefore, the trajectories for years 2000–2001 have been clustered according to their geographical coordinates using the MATLAB kmeans.m routine on the ensemble of trajectories. Clustering is a method that captures, in the case of

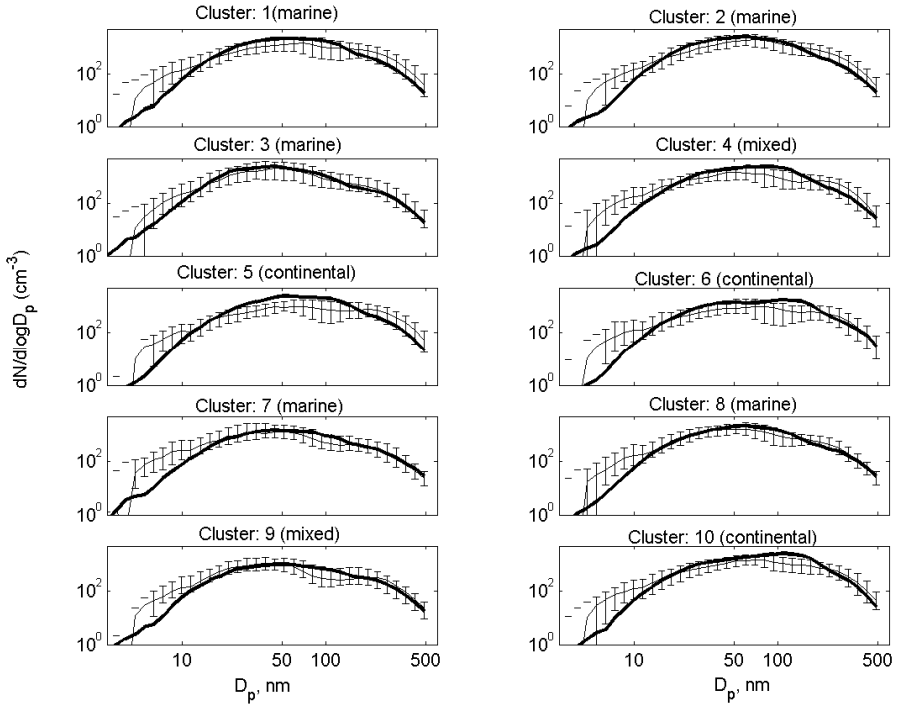

Fig. 8. Modelled and measured aerosol number size distribution data belonging to each on of the clusters in Fig. 7. Actual measurements at the receptor site Hyytiälä are presented as median and 25-th–75-th percentile ranges as indicated by the error bars. The thick black line corresponds to modelled median.

trajectory clustering, typical and distinct transport paths that the air follows before arriving to the receptor, maximizing the difference between the different clusters, while minimizing the difference between trajectories belonging to a certain cluster. The calculated clusters are shown in Fig. 7 as the cluster centroids (i.e. "average" trajectory of the different clusters) as well as the median height along each one of the clusters. 10 clusters have been considered in this analysis. The associated number size distributions for the period February–November for both years are shown in Fig. 8. Based on the centroids, cluster 1, 2, 3, 7, and 8 are predominantly of marine origin and thus referred to as Marine clusters, clusters 5, 6, and 10 are predominantly of continental origin (Continental clusters) and clusters 9 and 4 are considered to be of mixed marine-continental origin (Mixed clusters). The number of trajectories belonging to each cluster is shown in Table 3. All clusters show on average a descending transport pattern, but remain below 1000 m during most of the time.

During this period, the model performs well in most transport directions. Especially some of the marine trajectory clusters are associated with very good agreement between model and measurements (cf. Fig. 7, marine clusters 3, 7, 8, 9). The reason for just choosing February–November is that during December and January model performance is poor for most clusters, and would thus bias the otherwise satisfying agreement between model and measurements for the rest of the year. The cause of this generally poor representation of aerosol data during winter months is not well understood, but may be linked to more complicated real world winter time meteorology which CALM is not able to capture (e.g. stability, effect of clouds etc.) or inadequate representation of the wintertime sources.

In Figs. 9 and 10 the seasonal variation of the three dominating size ranges (or modes) of modeled and measured data for the receptor Hyytiälä during year 2000 and 2001 is shown. This comparison considers the accumulation mode size range ($D_p > 100$ nm, top frame), the Aitken mode size range (30 nm$< D_p <$100 nm, middle frame) and the nuclei size range ($D_p <$30 nm). Starting with the accumulation mode it is clear that the model captures the magnitude and trends of the accumulation mode in an excellent way during both years. Model and measurements follow each other very well for long periods of time. As with the monthly average size distributions previously described, the model representation does get worse during the end of the year. The modeled accumulation mode number concentration very of the higher than measured during the winter period. However, since both magnitude and trends are captured by the model, it is concluded that the way we represent sources and dominating processes is sufficiently accurate for the purpose of this study. This is an important finding since accumulation

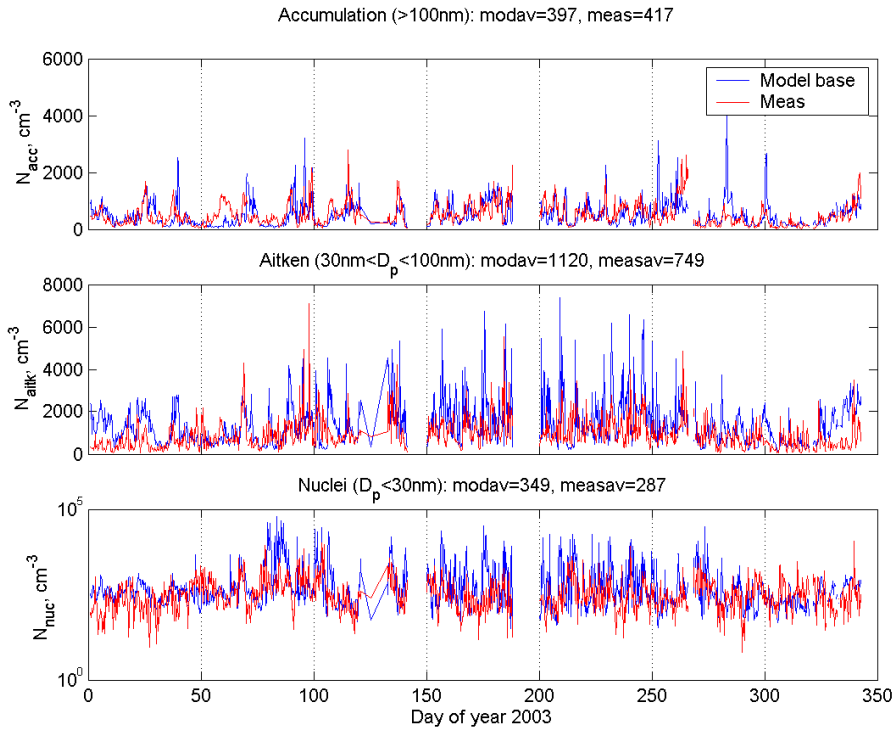

Fig. 9. Modeled and observed number concentration of accumulation mode particles (D_p >100 nm, top frame), Aitken mode particles (30< D_p <100 nm, middle frame) and nuclei mode (D_p <30 nm, bottom frame), cm^{-3}. Blue line show modeled data and red line shows measured concnetration. Hyytiälä, 2000.

mode provides the largest fraction of potential CCN, and thus an accurate description of this size range is of crucial importance for a proper determination of the important indirect aerosol effect on climate.

The seasonal variation of the Aitken mode (30< D_p <100 nm) number concentration through year 2000 is shown in the second frame of Figs. 9 and 10. As previously recognized, the model performs well especially during months 2–10, while the winter time agreement gets poorer as the model typically overestimates the Aitken mode concentration. The annual averages of modeled and measured Aitken mode concentration are 1190 cm^{-3} and 760 cm^{-3}, respectively. The model result is far patchier compared to the measured data, with several high peaks throughout the year. The general trend is however satisfying. One cause that could result in the discrepancy between the model and measurements is the fact that our current single trajectory approach will be very sensitive for local point sources. As described in the method part of this study, the mass based primary aerosol emissions are transformed into a fixed size distribution (Table 1), something that also could introduce an erroneous representation of the actual size distribution emitted, resulting in disagreement between the model and measurements.

The third frame of Figs. 9 and 10 shows the modeled and measured nuclei mode (D_p <30 nm) concentration. This figure is indicative of several interesting features related to the processes governing nucleation over Scandinavian boreal forests. Firstly, the model overestimates the average nuclei mode size range concentration (i.e. D_p <30nm). Annual modeled average is 390 cm^{-3} and measured annual average is 270 cm^{-3}. However, as reported in several previous studies (e.g. Dal Maso et al., 2005; Dal Maso et al., 2007, nucleation observed at Hyytiälä is generally associated with a pronounced seasonal pattern. Nucleation occurs rarely during winter months, followed by a spring maximum, and then again a summer minimum followed by another increase in nucleation during autumn. Previous discussions have invoked several possible explanations for this behavior. It is therefore highly interesting to notice that this seasonal trend is also captured by the model (in terms of abundance of nuclei mode particles), as is especially evident during year 2001 (Fig. 10). As shown in the figures both modeled and measured sub-30 nm particles show a good agreement with respect to the annual trend. Evident are the spring maximum, summer minimum and finally a smaller but significant increase during the autumn. In our model nucleation subsequent growth to detectable size is controlled by the balance between available condensing and nucleating vapors and the condensation and coagulation sink of the particles. Growth is favored during the summer month when the forest emits high amounts of BVOC (in our case represented by isoprene,

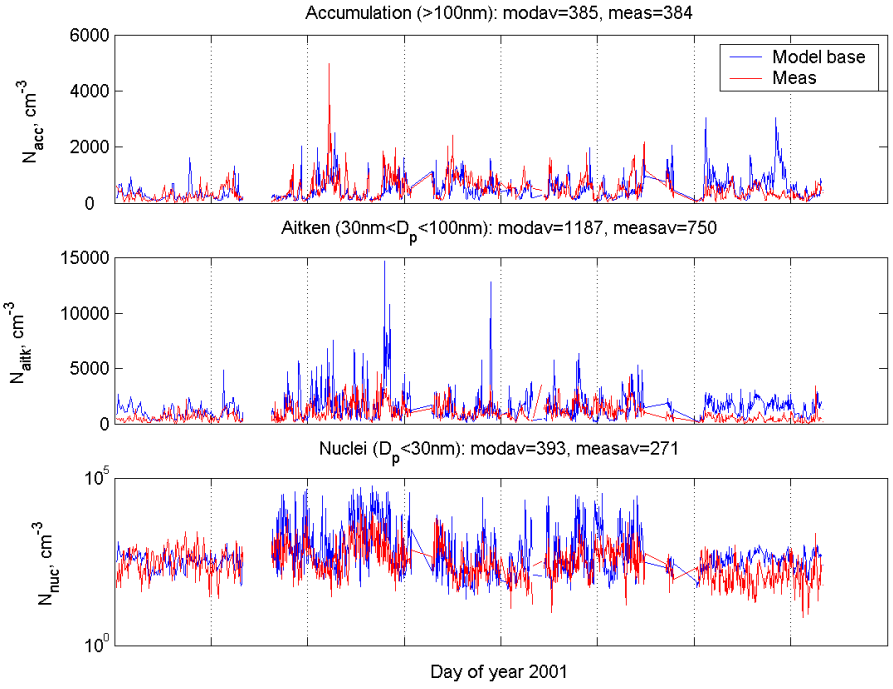

Fig. 10. Modeled and observed number concentration of accumulation mode particles (D_p >100 nm, top frame), Aitken mode particles (30< D_p <100 nm, middle frame) and nuclei mode (D_p <30 nm, bottom frame), cm^{-3}. Blue line show modeled data and red line shows measured concnetration. Hyytiälä, 2001.

monoterpenes and sesquiterpenes) while nucleation is governed by the concentration of H_2SO_4, which in turn is controlled by SO_2 emissions, condensation sink and insolation. During year 2000 also the modeled and measured trends of nuclei mode concentrations agree very well qualitatively.

It is further evident that CALM is able to reproduce the aerosol number and size with a good accuracy using only primary emissions and nucleation in the lower atmosphere and neglecting the influence of free troposphere (FT) nucleation and following entrainment. This contradicts to some extent the findings from earlier global model studies which have suggested that FT can account for up to 25% of the boundary layer particle number and CCN concentration (Merikanto et al., 2009).

3.2.2 Two case studies

Two highly resolved runs were performed to investigate how the model performs in air masses arriving from the clean marine sector and the polluted continental sector.

The clean period is represented by a period of 10 days in May 2000, associated with trajectories of marine origin that were advected to Hyytiälä. Nucleation is commonly observed over the boreal forest during spring when this type of air-mass transport dominates. As clean marine air is advected over Scandinavia, an abrupt change in sources occurs when going from the marine environment to forested areas which are proven to emit large amounts of BVOC (e.g. Simpson et al., 1995). As previously shown in Tunved et al. (2006a,b), nucleation followed by condensation of low or semi-volatile species is the process that most likely governs the evolution of number over the boreal forest during this type of transport. During the period investigated here, 1–10 May 2000, several nucleation events are indeed observed at the receptor site (Fig. 11). Pronounced nucleation events are observed 1, 2, 4, 6 and 7 May, corresponding to DOY 122, 123, 125, 127, 128. Traces of nucleation events are however also noticed an all other days except 3 May. In order to investigate how the model captures this type of transport in detail, CALM was run for the corresponding ten day period with a resolution of 1 h (i.e. the model was run along one individual trajectory every 1h through the studied period). The median modeled and 25-th–75-th percentile ranges of the number size distribution are shown in Fig. 13 (left frame). Both modeled and observed aerosol number size distributions share similar shape and magnitude, both showing a high concentration of nuclei mode particles as well as similar concentration of accumulation mode particles.. The model is able to reproduce the type of size distribution observed during this type of advection. However, as can be seen in Fig. 12, the modeled growth is slightly slower than the observed one, which is obvious from the shift of the peak in the Aitken mode size range. The explanation closest at hand is that the model underestimates the amount of condensing gases, which slows the growth relative

to the measurements. The model predicts a distribution peaking around 25 nm, while in the measurements the maximum is located around 35 nm. Agreement between measured and modeled number concentrations above 100 nm is good.

The lower frame of Fig. 11 shows is the modeled time evolution of the aerosol size distribution at Hyytiälä during the corresponding period. As can be seen, the model is often able to capture the temporal evolution of nucleation events during most of the days. The model does however suggest nucleation taking place also 3 May (although a rather weak nucleation), which is not seen in the observational data. Especially well captured are the particle formation and growth events during 1–2 May, 4–5 May and 6–7 May, although the model seems to overestimate the number of particles.

The polluted continental case was represented by 7 days in July 2001 (12–19 July), where trajectories arrived at Hyytiälä from SW in the beginning of the period, with a shift towards continental sources to the S-SE during the end of the period. The modeled and observed evolution of the size distribution at Hyytiälä is shown in Fig. 13. The period is characterized by a persistent accumulation mode located around 100 nm, with a rather small variation in size and concentration (Fig. 13, upper frame). This is a typical feature in continental air as observed at Hyytiälä. Furthermore, the data show low activity of new particle formation close to the receptor.

From Fig. 13, lower frame, it is seen that the model captures the general properties of the variation of the size distribution observed during the selected period. The modeled accumulation mode is however even more stable than observations, and some peaks indicating recent new particle formation are present in the observational data. This feature is lacking in the modeled data. The median modeled data during this case period is shown in the right frame of Fig. 12 together with measured median and 25-th–75-th percentile range of the data.

Comparing the two case studies, it is shown that the model produces widely separate size distributions comparing the two different extremes in source areas. The marine case is associated with a high number concentration and a size distribution shifted towards smaller sizes, i.e. traces of recent nucleation. It is also clear that the model seems to overestimate the nuclei mode concentration while underestimating the growth. This could very well be a result of the way the secondary organics are treated (i.e. treating first order products (15%) as very low volatile). This could result in higher concentration of small particles due to effective growth of the freshly formed particles to more or less stable sizes. This in turn could yield a larger condensation sink, which in turn hinders consecutive growth. The continental case is associated with lower number of particles, but the distribution is shifted towards the accumulation mode size range. The fact that these results agree well with observational data is encouraging.

3.2.3 Trace gases

In the following we show the agreement between measured and modeled sulfur dioxide (SO_2) and ozone (O_3). These gases are highly important controllers of both the nucleation rate and condensation growth (via H_2SO_4). Ozone in turn is an important oxidant itself, and is furthermore intimately linked to the production and cycling of reactive radicals (e.g. NO_3, OH, HO_2). Shown in (Fig. 14) is a comparison of measured and modeled [SO_2] and [O_3] at the SMEAR II station in Hyytiälä. In order to better see the general annual behavior, the data is presented as a 24 h running average to smooth out the presence of intermittent high peaks.

The annual average of measured SO_2 was found to be 130 ppt for year 2000. The modeled annual average was found to be 120 ppt. During 2001 the annual average of measured SO_2 was found to be 120 ppt, but the modeled annual average 160 ppt.

The annual average of measured O_3 was found to be 28 ppb for year 2000. The modeled annual average was found to be 27 ppb. During 2001 the annual average of measured O_3 was found to be 27 ppb, but with a modeled annual average of 26 ppb.

As can be seen in the figures both modeled and measured SO_2 show a pronounced seasonal variation, with maximum concentration during winter months. This is most likely the result of the combined effect of higher emissions, but also lower rate of photolytic degradation of SO_2 towards sulfuric acid. It is worth mentioning that the model appears to overestimate SO_2 during the winter. The seasonal variation of O_3 follows an opposite pattern, with maximum concentration during summer months, and minimum during winter, reflecting the opposite photochemical dependence of SO_2. The agreement between the model and measurement on the finer scale is not as good as for SO_2, but as shown by the annual average the magnitude of modeled and measured ozone agrees perfectly.

The modeled concentration of monoterpenes was found to be $\sim$80 ppt as an annual average, which is lower, but in the same range as measured literature values (e.g. (Hakola et al., 2009), which are typically below 100 ppt during winter and above 200 ppt during the middle of the summer. However, these measurements are often performed close to the canopy, whereas our modeled concentrations represent the average of the whole ML. Furthermore, we cannot exclude the possibility or stronger sinks due to higher than actual abundance of OH radicals. Since the emissions are temperature dependent, the highest emissions occur during summer time. Annual average for modeled isoprene was found to be 110 ppt, which is in the range, although slightly lower, compared to observed values.

Figure 15 shows the annual variation of different oxidants and condensable species in the model. Hydroxyl radical (OH) concentration reaches maximum during summer, with maximum concentrations around $10^7\,cm^{-3}$. Typical

Table 4. Comparison of annual average modal concentration for different sensitivity tests and base case simulation. Shown is the median for each sensitivity test. All units in cm^{-3}. Year 2000, Hyytiälä as receptor.

Mode	Base	No MT	No NUC	No Clouds	No Primary	All Continental	All Marine
Nucleation mode (D_p <30 nm)	390	510	180	390	110	310	390
Aitken mode (30< D_p <100 nm)	1190	1120	820	1360	465	970	1230
Accumulation mode (D_p >100 nm)	400	270	360	580	218	560	400

noon concentrations were around 2×10^6. This is well in the range, although slightly higher, of observations at Hyytiälä (Petaja et al., 2009, who observed 3–6×10^5 OH cm^{-3} during March–June).

Seasonal variation of nitrate radical is shown in the second frame of Fig. 15. The concentration is typically in the range of 10^7 cm^{-3}, but occasionally reaches above 10^8 cm^{-3}.

Sulfuric acid exhibits a typical seasonal variation, with maximum during summer months. Maximum concentrations is in the range of 1.0–1.5×10^7 cm^{-3} with an annual noon average of 1.8×10^6 cm^{-3}. This agrees well with observed concentrations at the Hyytiälä measurement station (Petaja et al., 2009).

The modeled concentration of condensable species at Hyytiälä resulting from monoterpene oxidation varies between 0.2–15×10^7 cm^{-3}. There are no available measurements to confront this result, but according to e.g. (Kulmala et al., 2001); (Spracklen et al., 2006) and references therein, investigations of new particle formation events at Hyytiälä indicate that the required concentration of condensable species to sustain the observed growth must be around 2×10^7–1.3×10^8 cm^{-3}. Thus, our results are in the lower range of these estimates.

3.3 Sensitivity tests

In this section we present the results for the sensitivity tests performed for the model. For these comparisons we have chosen year 2000. The main results are tabulated in Table 4, and will be referenced accordingly in the following text. The results of sensitivity tests with respect to nucleation, primary emissions, monoterpenes, clouds and precipitation and model initialization will be shown. The results will be discussed in terms of seasons and source regions of the air parcels simulated. In order to resolve the dependence of source regions we performed a clustering of the trajectories according to their typical advection paths. This will aid in the understanding of the importance of different processes at different locations/environments. The clusters for 2000 are shown in Fig. 16.

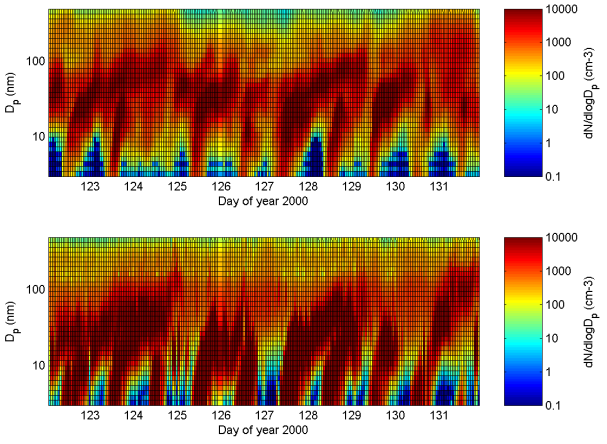

Fig. 11. Obsereved (top frame) and modeled (bottom frame) size distribution evolution. Hyytiälä, 1–10 May 2000.

3.3.1 Nucleation and primary emissions

In the model, addition of aerosols by number is controlled by either primary emitted particles (as described under Sect. 2.4.3) or nucleation and consecutive growth. The primary emissions are confined to predefined size ranges, while nucleation always start with sub-nm particles formed from the gas phase. Since the number is relevant for both health and climate issues related to the atmospheric aerosol, it is of interest to investigate how the model responds to perturbations of these number concentration controlling processes. In this section we present results derived from three different sensitivity tests, one with nucleation completely disabled, one with an activation coefficient representing the minimum A derived at Hyytiälä (4×10^{-7} s^{-1}) and one with a maximum empirically derived A (6×10^{-6} s^{-1}). These numbers are taken from Riipinen et al. (2007) who compared the first order activation nucleation coefficient for different locations. In the base case, as mentioned previously, we assume a flat coefficient A of 2×10^{-6} s^{-1}. Additional to these tests we also investigate the response to a complete cancellation of primary emissions.

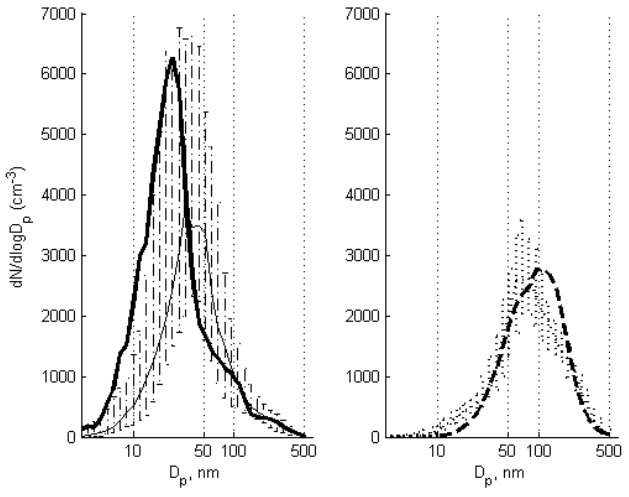

Fig. 12. Modelled and measured number size distribution. Measurment data shown as median and 25-th–75-th percentile range. Model data represented by the thick solid line. Left frame, marine transport, Hyytiälä 1–10 May 2000. Right frame, continental transport, Hyytiälä 12–19 July 2001.

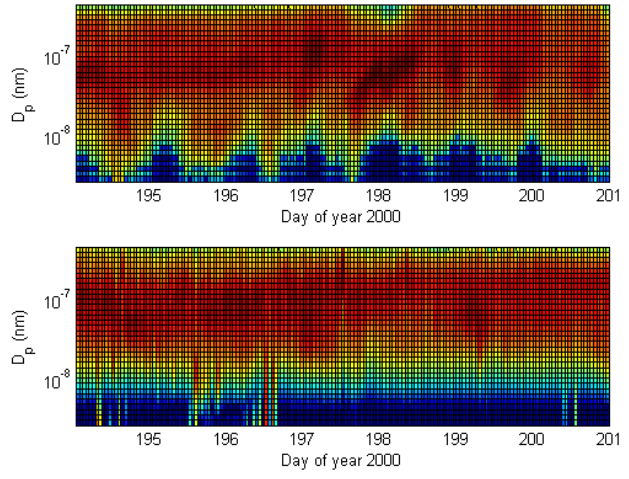

Fig. 13. Obsereved (top frame) and modeled (bottom frame) size distribution evolution. Hyytiälä, 12–19 July 2001.

By applying the range of values of A to two different simulations, only very small changes in the final average size distributions were noticed (not shown). This suggests that the exact value of the nucleation coefficient is insignificant for modeling on this scale. This conclusion is valid even with an order of magnitude difference in A between the two runs. Instead, beside the nucleation itself, the ability of the particles to grow in the environment in which they are formed is of crucial importance. This ability in turn is related to the condensation sink of pre-existing particles as well as the rate of coagulation of the freshly formed particles.

Figure 17 shows the winter (October–March) and summer (April–September) average size distributions for the run with nucleation disabled and the base case distribution. Both are for year 2000. As can be clearly seen, nucleation provides the largest addition of aerosol number during the summer months, while the runs with no nucleation during the winter period result in virtually the same aerosol number size distribution as the base case. This is well in agreement with previous findings, showing nucleation to occur preferentially during the spring-autumn period, indicating the dependence on photochemical processes governing nucleation. As shown in Table 4, with nucleation disabled, the annual average of nuclei mode particles is decreased from 390 to 180 cm^{-3}, the Aitken mode is reduced from 1190 to 820 cm^{-3} and the accumulation mode is reduced from 400 to 360 cm^{-3}. The accumulation mode typically represents the amount of available CCN, and since nucleation provides ∼10% of these particles it is clear that nucleation provides a substantial contribution to potential CCN's, also as an annual average. As shown, this contribution is most pronounced during the summer period (April–September). The presence of nuclei mode particles also in the simulation where nucleation is turned off is explained by the primary emissions, contributing to sub 30 nm particles.

More interestingly, as shown in Fig. 18, the role of nucleation differs largely between different clusters (Fig. 16). This figure shows the summer time base case runs, together with runs with nucleation disabled. As can be seen, nucleation has a large impact on sub-100 nm particles in clusters 2, 4, 6, 9 and 10. Clusters 4, 6, 9 and 10 are typically associated with marine air advection from north and cluster 2 centroid is directed over continental sources oriented NE of Hyytiälä. The least dependence of final size distribution on nucleation is observed in clusters 1, 5 and 8. These clusters arrive from continental sources, and both base case and the run with nucleation disabled are nearly identical. Remaining clusters share both continental and marine sources, and consequently there are some differences between no nucleation case and base case. These findings indicate that nucleation is an important contributor to the total aerosol number at Hyytiälä only when advection occurs from clean regions. The fact that nucleation preferentially occurs in clean, polar air masses has been known for several years (Boy et al., 2005; Sogacheva et al., 2008). What is interesting with these results is however, that even if nucleation is disabled over the continental region, this does not have a large impact on the resulting size distribution observed in Hyytiälä. These findings qualitatively agree with the results and discussions presented by Spracklen et al. (2006), using the global model GLOMAP. In clean regions, nucleation is a significant contributor to aerosol number, while in the outflow of large pollution sources it is not.

In Fig. 19 we show the summer and winter distributions resulting from base case simulations and simulations with all primary sources disabled. As can be seen, the lack of primary

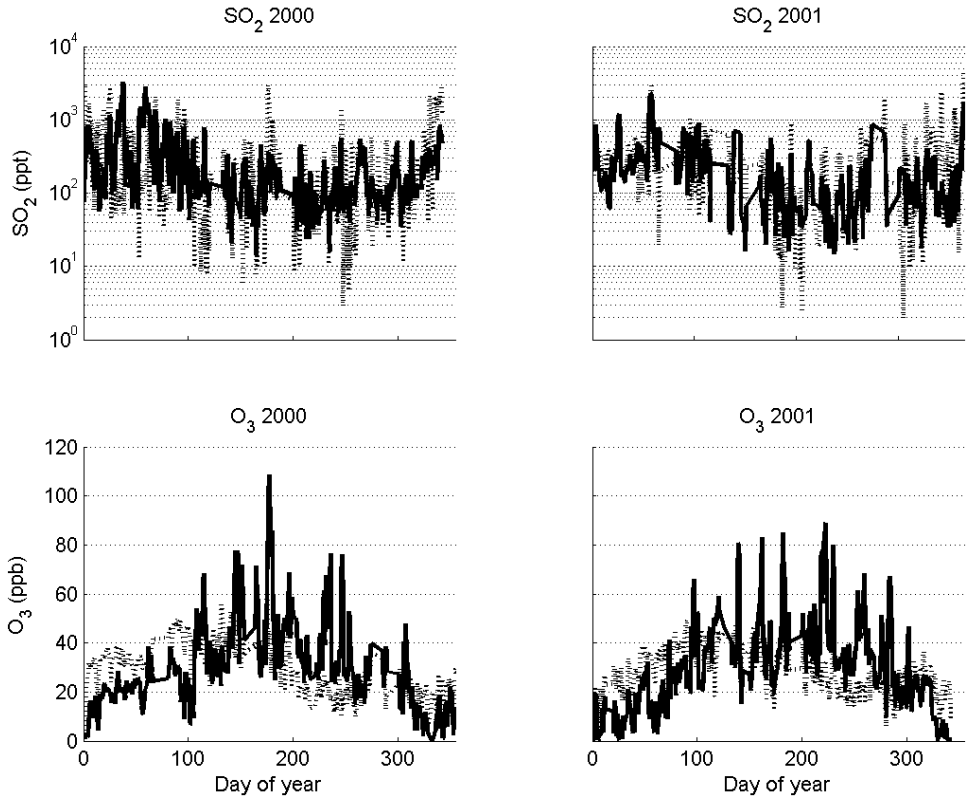

Fig. 14. Measured and modeled SO_2 concentrations in ppt (top frames) and measured and modeled O_3 concentration in ppb through years 2000–2001 (bottom frames), Hyytiälä, 2000–2001.

emissions affects both the summer and winter periods, although the difference is most pronounced for the winter period. This is opposite to the dependence on nucleation. From Fig. 20 it is also obvious that the clusters with the largest continental influence (i.e. cluster 1, 5 and 8) are most sensitive to the primary emissions (although insensitive to nucleation). This means that primary emissions have a much larger impact than nucleation during these transport conditions. Also interesting to notice is that the clusters that were most prone to be influenced by nucleation, respond quite differently compared to their continental counterparts. This is especially evident in clusters 9 and 10, where the reduced primary emissions apparently lead to an overall higher concentration in the nuclei mode size range (here defined as particle with D_p <30 nm). This is possibly the result of lower condensation sink associated with the runs neglecting primary emissions, something that favors nucleation and subsequent detectable growth. During the winter period, each cluster is subject to reduction in particle number due to the absence of nucleation.

In summary this means that particle number is governed by different processes in polluted and clean environments, i.e. primary and secondary formation, respectively.

3.4 BVOC

In the model we apply a stochiometric yield of 15% condensable species from primary oxidation of MT (as represented by α-pinene). By cancelling out monoterpene emissions we now investigate the role of the dominating source of BVOC in the model. As a response in terms of annual average of the three different modes we notice a reduction in accumulation mode (400 and 270 cm^{-3} for base case and sensitivity, respectively), a slight decrease in Aitken mode (1190 and 1120 cm^{-3}) and an increase in nuclei mode particles (390 and 510 cm^{-3}). The reduction of accumulation mode particles reflects the fact that less condensable species are available to support growth into larger sizes. The insignificant change in the Aitken mode however is argued to be the combined result of more frequent nucleation due to reduction of the condensation sink combined with the fact that primary emissions largely contribute to this size range, and also that particles emitted in this size range do not grow into the accumulation mode size range. The increase of nuclei mode particles is explained by the reduced CS. More particles are formed on average via nucleation, although they grow much slower. Figure 21 confirms this, by showing winter and summer average size distributions for base case and runs with no

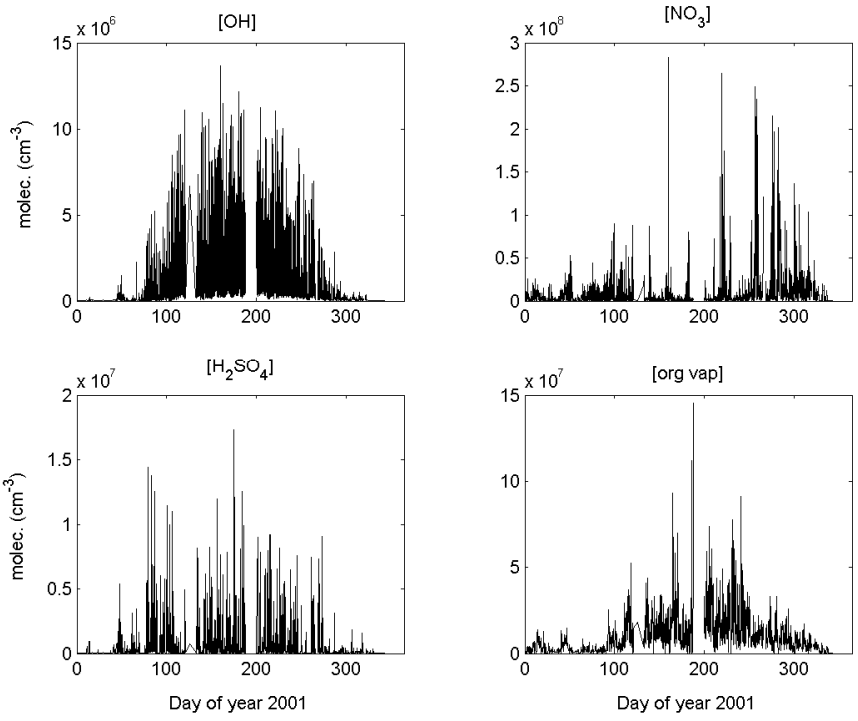

Fig. 15. Modeled concnetrations of hydroxyl radical (OH, top left), nitrate radical (NO_3, top right), sulfuric acid (H_2SO_4, lower left) and condensable organics (lower right). All units as cm^{-3}, Hyytiälä 2001.

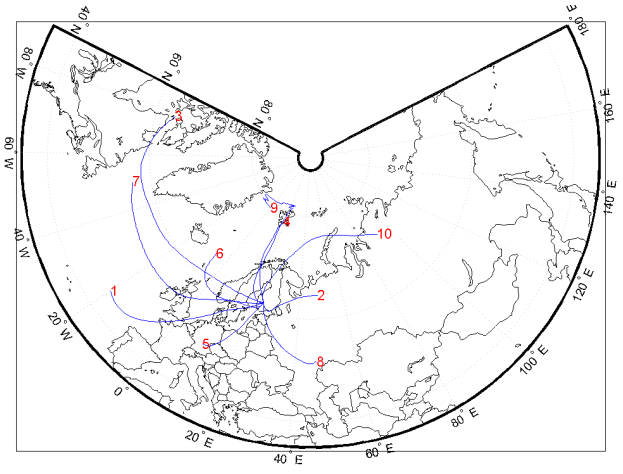

Fig. 16. Trajectory clusters centroids calculated for year 2000. Cluster number is indicated at the end of each centroid.

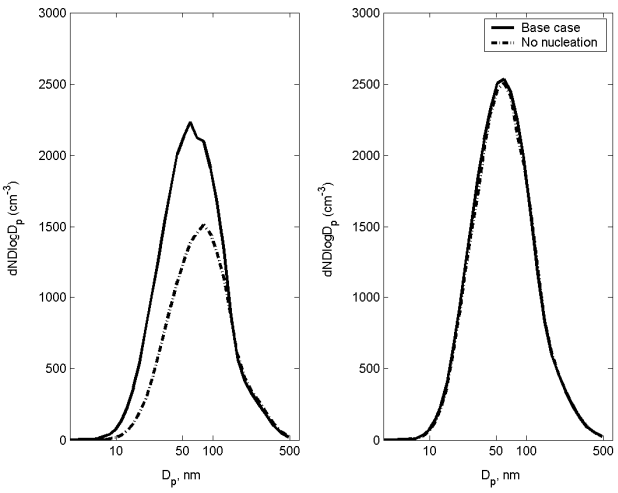

Fig. 17. Comparison between model base case and runs with nucleation disabled. Two periods considered, summer (April-September, right frame) and winter (October–March, left frame), Hyytiälä, 2000.

MT emissions. During both seasons, the number size distribution is shifted towards smaller sizes. This effect is most pronounced during the summer time when MT emissions are expected to be high. The shift towards smaller sizes is evident in all transport directions, but most pronounced in cluster 9, where the sizes are not only smaller, but the number of nuclei mode particles is far higher without MT emissions as compared to the base case (not shown). MT emissions are thus argued to be an important contributor to the growth of both nucleated and primarily emitted particles into CCN sized particles.

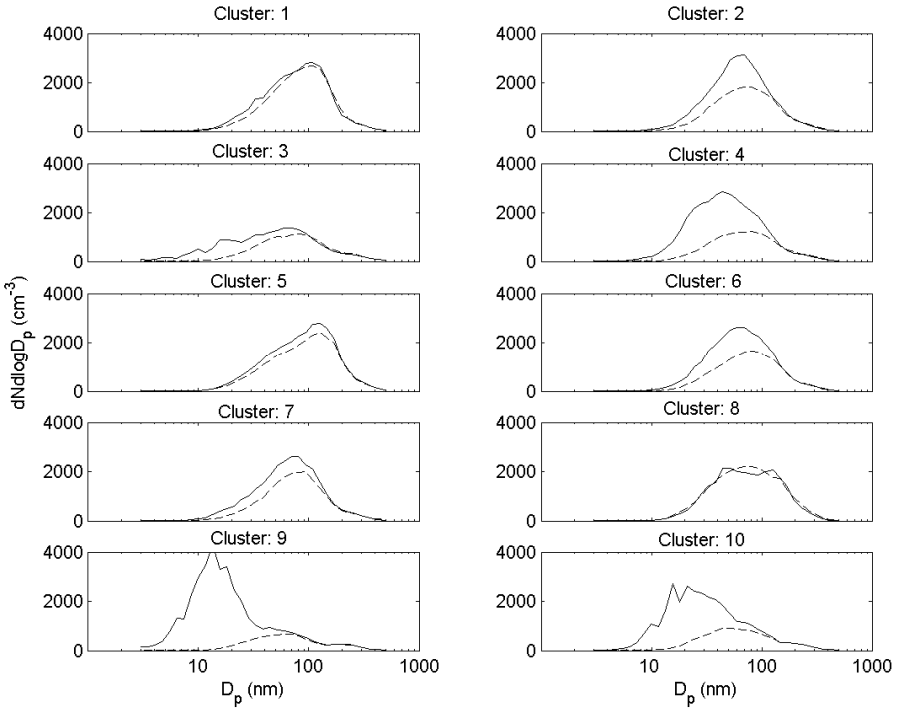

Fig. 18. Comparison between model base case and runs with nucleation disabled per cluster. Dashed line indicate the duns with nucleation disabled, full lines represent bas case conditions, Hyytiälä, 2000.

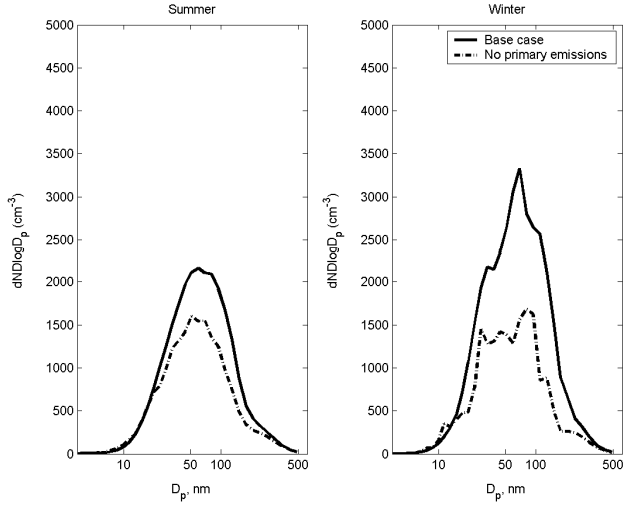

Fig. 19. Comparison between model base case and runs with primary emissions disabled. Two periods considered, summer (April–September, right frame) and winter (October–March, left frame). Hyytiälä, 2000.

3.5 Initial conditions

In order to assure that the model result isn't biased by the initial conditions, the role of the starting size distribution and initial values of O_3 and NO_x was investigated in three separate tests. Therefore, three different setups were chosen: one where all simulations are initialized with the continental type size distribution, one where all runs were initialized with the marine type size distribution and finally one test where initial O_3 was set to 25 ppb (i.e. 10 ppb's less than base case conditions) and NO_x was set to 0.1 (i.e. 5 times less than base case conditions). The results are shown in Figs. 22–23 for continental and marine starting distributions, respectively. As can be seen, if the model is initialized with only continental size distributions, a shift of both wintertime and summer time average size distributions towards larger sizes is obvious. However, on closer inspection with respect to the cluster orientations, it was concluded that the difference is only pronounced in the clean, marine clusters 4, 9, 10 (not shown). This is interpreted as the lifetime of the starting distribution in these cases being too long for the model to equilibrate to marine conditions. However, if all initial size distributions were substituted with their marine counterparts, negligible change compared to base case conditions was observed. This means that the source strength in polluted areas in principle is strong enough to allow for equilibration to continental conditions rather rapidly.

The results from the runs with lower than base case concentration ozone and NO_x, the evolution of OH and $NO_2 + NO$ as average along the trajectories of year 2000 is shown in Fig. 24. When choosing to initialize with lower NO_x and ozone, one might expect at corresponding change

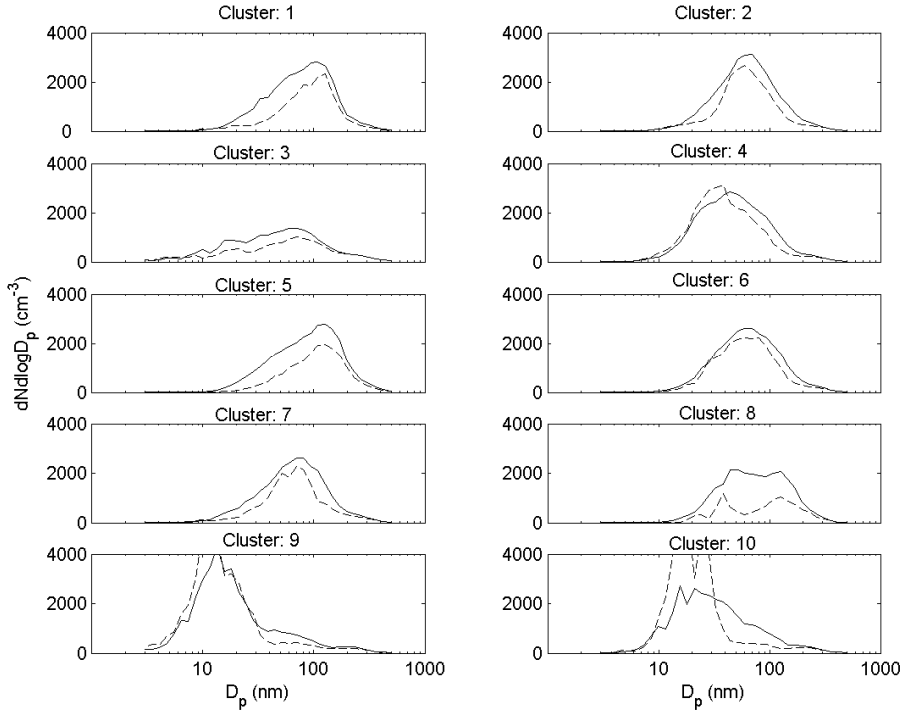

Fig. 20. Comparison between model base case and runs with primary emissions disabled per cluster. Dashed line indicate the duns with primary emissions disabled, full lines represent bas case conditions, Hyytiälä, 2000.

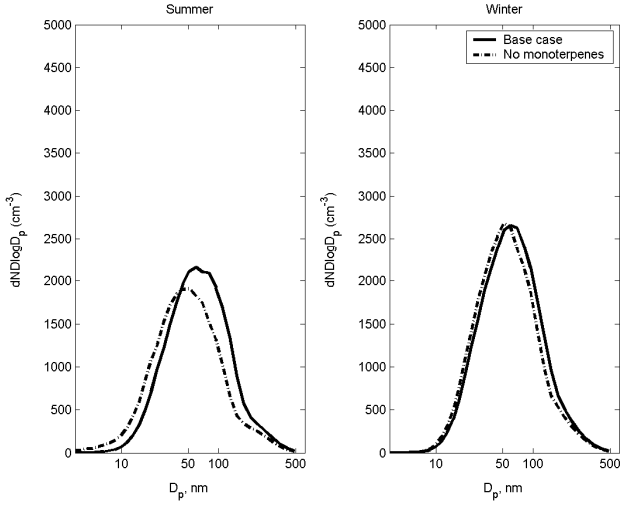

Fig. 21. Comparison between model base case and runs with monoterpene emissions disabled. Two periods considered, summer (April–September, right frame) and winter (October–March, left frame), Hyytiälä, 2000.

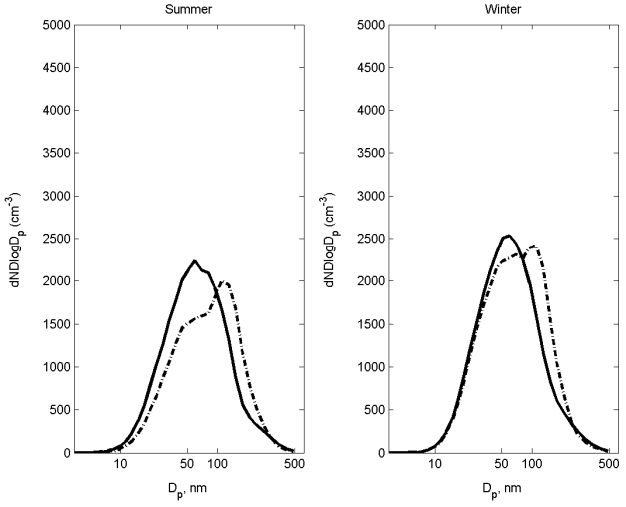

Fig. 22. Comparison between model base case and runs initialized with continental distributions only. Two periods considered, summer (April-September, right frame) and winter (October–March, left frame), Hyytiälä 2000.

in both ozone and OH concentration along the trajectories, and that this in turn will influence the oxidation potential and thus production of condensable species. In this test the initial concentration of O_3 is 10ppb less than the concentration in the base case runs and the ozone recovers slowly during the length of the model run, and on average, at the end of the runs, the difference is less than 4 ppb (not shown). However, OH concentration and $NO_2 + NO$ show a much more rapid

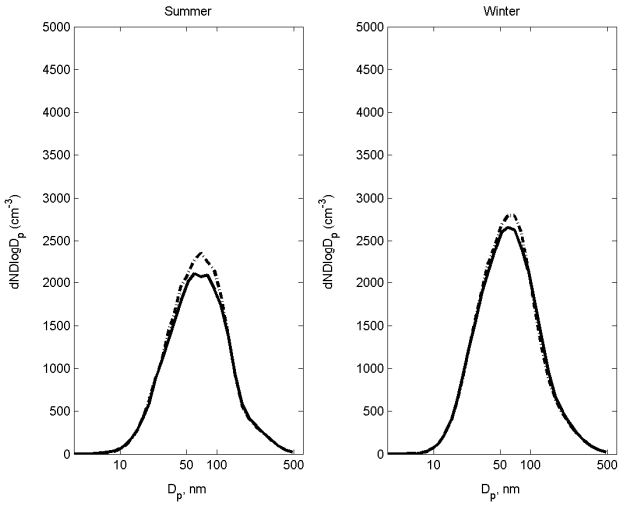

Fig. 23. Comparison between model base case and runs initialized with marine distributions only. Two periods considered, summer (April-September, right frame) and winter (October–March, left frame), Hyytiälä, 2000.

recovery, and it is shown in Fig. 24 that NO_x for the both types of simulation gets comparable after ∼80 h, and then follow each other until arrival at the receptor. When using the lower initial values of ozone and NO_x OH requires slightly more time to recover to base case values, and gets comparable to the base case runs (at an average of $\sim 4 \times 10^{-5}$ cm^{-3}) after approx. 120 h. However, the change in final size distribution as a result hereof is very minor and not shown. This test shows, that the initialization of the model with proper gas phase concentrations is important to get an accurate description of the evolution of species such as ozone, but show at the same time that the final aerosol size distribution is largely unaffected by these moderate changes in ozone and NO_x.

3.6 Clouds and precipitation

The role of clouds and precipitation was investigated by simply cancelling out clouds and rain in the model scheme. The largest relative effect of this was an increase of the accumulation mode number concentration (Table 4) which increases from 400 to 580 cm^{-3} while the Aitken mode increases from 1190 to 1360 cm^{-3}. Somehow, the nuclei mode annual average concentration remained unaffected. This probably reflects the fact that although the condensations sink increases, SO_2 will be more abundant due to less scavenging by the clouds and precipitation, thus providing more nucleating material in terms of H_2SO_4. This indicates that clouds do play an important role in the model, and thus are necessary to achieve the observed good agreement between model and measurements during the studied period. The change is most pronounced during the summer months, although of similar magnitude during winter. There was no clear (relative) dependence on source regions when performing the analysis per cluster, but instead all clusters were associated with a substantial increase in the Aitken-accumulation mode size range.

3.6.1 Transport in or above mixing layer

The simplified model set-up used in this study utilize the coordinates of the trajectories to describe the movement of a quasi-1-D column consisting of a mixing layer (ML) and residual layer (RL) compartment. Thus, the model describes how the model compartments move along the latitude-longitude coordinates until the receptor station (in this case Hyytiälä) is reached. As transport path and speed may vary significantly with altitude, trajectories travelling at on average higher altitudes may not always yield a fair representation of experienced sources and transport speed of the air in the boundary layer above the receptor. On average during the simulations, the air-parcel spend 74% (or 160 h of 216 h total transport) of the time within the mixing layer. In order to test the validity of our model setup we divide the model output into two groups, one of which the air spends more than 160 h in ML and one group that spends less than 160 h in the ML. for this test we utilize only trajectories calculated for year 2000.

For the trajectories spending more than 160 h in the ML, the simulated average of the accumulation mode number concentrations was 480 cm^{-3}, compared to measured average of 418 cm^{-3}. Corresponding values for the Aitken mode was found to be 1185 cm^{-3} and 698 cm^{-3} for modeled and measured concentration, respectively. Modelled nuclei mode concentration was found to be 314 cm^{-3} compared to the measured average of 245 cm^{-3}.

In the case of less time spent in ML, the simulated average of the accumulation mode number concentration was 322 cm^{-3}, compared to measured average of 368 cm^{-3}. Corresponding values for the Aitken mode was found to be 1221 cm^{-3} and 837 cm^{-3} for modeled and measured concentration, respectively. Modelled nuclei mode concentration was found to be 468 cm^{-3} compared to the measured average of 326 cm^{-3}.

Thus, in the case of dominating ML transport, we slightly over predict the accumulation mode concentration, and in the cases with less ML transport we under predict the accumulation mode number concentration. This result in, most likely due to the reduced condensation sink, more nuclei mode particles in the case of less ML transport as compared to cases dominated by ML transport. The differences between the two cases are typically small and both high ML and low ML transport conditions result in a good agreement between modeled and measured number concentrations. In order to avoid this kind of bias, a more thorough description of the vertical structure and transport would be required, and this is unfortunately beyond the scope of this study and model framework.

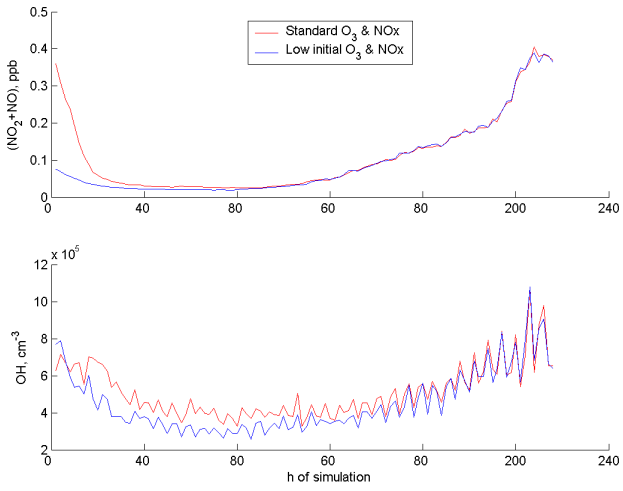

Fig. 24. Comparisons of runs when using base case and modified initial gas phase concentrations of NO_x and ozone. Top frame shows the average evolution of $NO + NO_2$ along the trajectories for the low ozone (25ppb) and low NO_x (0.1 ppb) (blue curve) compared with base case initialisation (35 ppb ozone and 0.5 ppb NO_x, red curve). Bottom frame, same as above but evolution of OH is depicted.

4 Summary and conclusions

In this study we have presented a new Chemical and Aerosol Lagrangian Model (CALM) that describe the evolution of particle distribution and chemical key species along trajectories and selected receptor sites. The model performs quickly enough to be run on standard PC units, and supplies users with an easy tool to investigate the relative role of aerosol dynamic processes controlling the appearance and fate of particles in the atmosphere. The model incorporates the most central aspects of the aerosol dynamics in both the dry and wet phase of the atmosphere and does as shown provide an excellent tool for determining dominating processes with a large degree of transparency and accessibility.

Considering the model performance, CALM is able to capture the most prominent aspects of the observed aerosol at the Hyytiälä measurement station. This statement is valid, with the exception of the winter period, when the model performs poorly. The explanation for this remains open, but it may relate to a more complicated meteorology that is not captured by the trajectory model used, e.g. stratification of the lower atmosphere. It could also relate to a seasonality of the sources that is not well captured by the emission module. Measured and modeled accumulation mode number concentrations are similar with respect to both magnitude and seasonal trends. This applies also to the modeled and measured nuclei mode number concentration. Investigation of the model results versus actual observations provided a mechanistically sound explanation/description of the seasonal variation of nuclei mode particles, highlighting the importance of balance between the generation of nucleating and condensable species and their corresponding condensation sink. The model, however, seems to overestimate the Aitken mode number concentration. The poorer agreement between the measured and modeled Aitken mode particle number may be related to the way primary emissions are described. The model also performs satisfactorily in comparing either size distribution in relation to different months or different source regions and transport routes. This indicates that the model can cope with different environments and source regions and more importantly, that the model provides a qualitative and quantitative balance between the governing processes, something that is shown by the satisfying agreement between observed and measured sulfur dioxide and the fair agreement between modeled and measured ozone, as well as reasonable representation of the concentrations of monoterpenes, isoprene, radicals and sulfuric acid.

In addition, the sensitivity of the model to different processes has been investigated in detail. The overall findings suggest that the processes are well balanced. The sensitivity tests have also provided insight into the processes governing the aerosol as observed at the Hyytiälä measurement station. These conclusions include, but are not limited to:

- Nucleation is important for the provision of particle number in clean air masses only. Under continental, polluted conditions primary emissions provide most particle number.

- The model result (as represented by the receptor site Hyytiälä) proved virtually insensitive over an order of magnitude range of nucleation coefficient (4×10^{-7}–$6 \times 10^{-6}\,s^{-1}$, activation theory, J~$[H_2SO_4]$). This suggests that other processes than nucleation rate itself limit the provision of stable particles via this nucleation mechanism within this range of nucleation coefficients. This could for example be availability of condensable species and/or rate of coagulation of freshly formed particles. This finding eases the selection of A for modelers (The nucleation activation theory coefficient A has been shown to vary between different environments (Riipinen et al., 2007).

- Monoterpenes are an important contributor to particles above 100 nm since their oxidation products facilitates growth of particles over the entire size range. This indicates that monoterpenes may indirectly influence the radiation budget of the atmosphere. The role of monoterpenes was found to be most pronounced in the clean transport sectors of Hyytiälä.

- Clouds, as described in CALM, do play an important role in regulating especially the accumulation mode concentration. By cancelling clouds and precipitation, the number of accumulation mode particles is substantially increased.

The model has been extensively tested and the results of these tests have proved the model to perform reasonably well. It has not been within the scope of this study to extend the testing to other sites than the Hyytiälä station. As with most model approaches, also the presented approach is associated with good and less good approximations. Thus, the model approach is associated with a number of advantages and disadvantages which are outlined below.

The model can with reasonable computational demand cope with a high level of detail of the aerosol dynamic processes in the dry atmosphere. CALM can be used with an arbitrary number of sections/compositions without significant loss in computational efficiency (within reasonable limits).

The model is easily adoptable to different sites and locations. CALM is furthermore easily expandable to test different chemical schemes and dynamic process descriptions and is thus suitable for use as an evaluation tool for aerosol dynamic process parameterizations in regional and global models.

However, Lagrangian box-models obviously suffer, by necessity, from several more or less coarse parameterizations. In the case of CALM, the most central disadvantages are the rudimentary description of vertical and horizontal mixing and exchange. Two layer representation of model space could be unsuitable for certain locations. This may lead to unrealistic results, especially if the modeled receptor is located close to polluted regions with large density of point sources. However, the average result of simulations over longer periods of time (weeks-months) likely reflects the actual source field experienced over the same period. This is evident from the good agreement between the model and measurements, especially looking at monthly and annual averages. Furthermore, the method is likely to be suitable for regions surrounded by homogenous source fields similar to the boreal region itself. It is undeniably doubtful that the often good agreement of hourly simulated and measurement data (especially considering the accumulation mode concentration) would be coincidental only. Also, the validity of the simplified cloud description/treatment in the model must be tested more extensively, e.g. for other sites and locations. The model only considers washout processes (i.e. below cloud scavenging), with rain coming from clouds formed above the modeled column. This approximation is likely valid for rain from frontal type clouds (e.g. nimbostratus clouds), while not being the preferred solution for convective type precipitation with boundary layer air actively partaking in the cloud and precipitation forming processes. Nevertheless, the semi-empirical parameterization used implicitly takes into account both washout and rainout processes since it is based on the observed rate of change of boundary layer aerosol concentration and its relation to precipitation rate.

It remains a future task to better validate the presented process description, especially considering the model performance over longer time periods and over larger spatial scales. Ongoing measurement initiatives will support this future work by supplying relevant data required to validate the model (especially the EUCAARI- and EUSAAR-programs).

Acknowledgements. This work has been supported by Swedish Research Council, EUCAARI (European Integrated project on Aerosol Cloud Climate and Air Quality interactions) No 036833-2 and EUSAAR and the European Community – Research Infrastructure Action under the FP6 "Structuring the European Research Area" Programme, EUSAAR Contract No. RII3-CT-2006-026140.

The insightful comments by Ilona Riipinen and an anonymous reviewer significantly helped to improve the manuscript.

Edited by: M. Kulmala

References

Alados-Arboledas, L., Olmo, F. J., Alados, I., and Perez, M.: Parametric models to estimate photosynthetically active radiation in Spain, Agr. Forest. Meteorol., 101, 187–201, 2000.

Andersson-Skold, Y. and Simpson, D.: Secondary organic aerosol formation in northern Europe: A model study, J. Geophys. Res.-Atmos., 106, 7357–7374, 2001.

Boy, M., Kulmala, M., Ruuskanen, T. M., Pihlatie, M., Reissell, A., Aalto, P. P., Keronen, P., Dal Maso, M., Hellen, H., Hakola, H., Jansson, R., Hanke, M., and Arnold, F.: Sulphuric acid closure and contribution to nucleation mode particle growth, Atmos. Chem. Phys., 5, 863–878, doi:10.5194/acp-5-863-2005, 2005.

Capaldo, K. P., Kasibhatla, P., and Pandis, S. N.: Is aerosol production within the remote marine boundary layer sufficient to maintain observed concentrations? J. Geophys. Res.-Atmos., 104, 3483–3500, 1999.

Chameides, W. L. and Stelson, A. W.: Aqueous-phase chemical processes in deliquescent sea-salt aerosols – a mechanism that couples the atmospheric cycles of s and sea salt, J. Geophys. Res.-Atmos., 97, 20565–20580, 1992.

Dal Maso, M., Kulmala, M., Riipinen, I., Wagner, R., Hussein, T., Aalto, P. P., and Lehtinen, K. E. J.: Formation and growth of fresh atmospheric aerosols: eight years of aerosol size distribution data from SMEAR II, Hyytiala, Finland, Boreal. Environ. Res., 10, 323–336, 2005.

Dal Maso, M., Sogacheva, L., Aalto, P. P., Riipinen, I., Komppula, M., Tunved, P., Korhonen, L., Suur-Uski, V., Hirsikko, A., Kurten, T., Kerminen, V. M., Lihavainen, H., Viisanen, Y., Hansson, H. C., and Kulmala, M.: Aerosol size distribution measurements at four Nordic field stations: identification, analysis and trajectory analysis of new particle formation bursts, Tellus B, 59, 350–361, 2007.

Danilin, M. Y., Ebel, A., Elbern, H., and Petry, H.: Evolution of the concentrations of trace species in an aircraft plume – trajectory study, J. Geophys. Res.-Atmos., 99, 18951–18972, 1994.

Dentener, F., Kinne, S., Bond, T., Boucher, O., Cofala, J., Generoso, S., Ginoux, P., Gong, S., Hoelzemann, J. J., Ito, A., Marelli, L., Penner, J. E., Putaud, J.-P., Textor, C., Schulz, M., van der Werf, G. R., and Wilson, J.: Emissions of primary aerosol and precursor gases in the years 2000 and 1750 prescribed data-sets for AeroCom, Atmos. Chem. Phys., 6, 4321–4344, doi:10.5194/acp-6-4321-2006, 2006.

Griffin, R. J., Cocker, D. R., Seinfeld, J. H., and Dabdub, D.: Estimate of global atmospheric organic aerosol from oxidation of biogenic hydrocarbons, Geophys. Res. Lett., 26, 2721–2724, 1999.

Grini, A., Korhonen, H., Lehtinen, K. E. J., Isaksen, I. S. A., and Kulmala, M.: A combined photochemistry/aerosol dynamics model: model development and a study of new particle formation, Boreal. Environ. Res., 10, 525–541, 2005.

Guenther, A., Hewitt, C. N., Erickson, D., Fall, R., Geron, C., Graedel, T., Harley, P., Klinger, L., Lerdau, M., McKay, W. A., Pierce, T., Scholes, B., Steinbrecher, R., Tallamraju, R., Taylor, J., and Zimmerman, P.: A Global-model of natural volatile organic-compound emissions, J. Geophys. Res.-Atmos., 100, 8873–8892, 1995.

Guenther, A. B., Zimmerman, P. R., Harley, P. C., Monson, R. K., and Fall, R.: Isoprene and monoterpene emission rate variability - model evaluations and sensitivity analyses, J. Geophys. Res.-Atmos., 98, 12609–12617, 1993.

Hakola, H., Hellen, H., Tarvainen, V., Back, J., Patokoski, J., and Rinne, J.: Annual variations of atmospheric VOC concentrations in a boreal forest. Boreal. Environ. Res., 14, 722–730, 2009.

Hakola, H., Tarvainen, V., Back, J., Ranta, H., Bonn, B., Rinne, J., and Kulmala, M.: Seasonal variation of mono- and sesquiterpene emission rates of Scots pine, Biogeosciences, 3, 93–101, 2006.

Kettle, A. J., Andreae, M. O., Amouroux, D., Andreae, T. W., Bates, T. S., Berresheim, H., Bingemer, H., Boniforti, R., Curran, M. A. J., DiTullio, G. R., Helas, G., Jones, G. B., Keller, M. D., Kiene, R. P., Leck, C., Levasseur, M., Malin, G., Maspero, M., Matrai, P., McTaggart, A. R., Mihalopoulos, N., Nguyen, B. C., Novo, A., Putaud, J. P., Rapsomanikis, S., Roberts, G., Schebeske, G., Sharma, S., Simo, R., Staubes, R., Turner, S., and Uher, G.: A global database of sea surface dimethylsulfide (DMS) measurements and a procedure to predict sea surface DMS as a function of latitude, longitude, and month, Global Biogeochem. Cy., 13, 399–444, 1999.

Korhonen, H., Lehtinen, K. E. J., and Kulmala, M.: Multicomponent aerosol dynamics model UHMA: model development and validation, Atmos. Chem. Phys., 4, 757–771, doi:10.5194/acp-4-757-2004, 2004

Kulmala, M., Hameri, K., Aalto, P. P., Makela, J. M., Pirjola, L., Nilsson, E. D., Buzorius, G., Rannik, U., Dal Maso, M., Seidl, W., Hoffman, T., Janson, R., Hansson, H. C., Viisanen, Y., Laaksonen, A., and O'Dowd, C. D., Overview of the international project on biogenic aerosol formation in the boreal forest (BIOFOR), Tellus B, 53, 324–343, 2001.

Kulmala, M., Laaksonen, A., and Pirjola, L.: Parameterizations for sulfuric acid/water nucleation rates, J. Geophys. Res.-Atmos., 103, 8301–8307, 1998.

Kulmala, M., Lehtinen, K. E. J., and Laaksonen, A.: Cluster activation theory as an explanation of the linear dependence between formation rate of 3 nm particles and sulphuric acid concentration, Atmos. Chem. Phys., 6, 787–793, doi:10.5194/acp-6-787-2006, 2006.

Laakso, L., Gronholm, T., Rannik, U., Kosmale, M., Fiedler, V., Vehkamaki, H., and Kulmala, M.: Ultrafine particle scavenging coefficients calculated from 6 years field measurements, Atmos. Environ., 37, 3605–3613, 2003.

Laaksonen, A., Kulmala, M., O'Dowd, C. D., Joutsensaari, J., Vaattovaara, P., Mikkonen, S., Lehtinen, K. E. J., Sogacheva, L., Dal Maso, M., Aalto, P., Petäjä, T., Sogachev, A., Yoon, Y. J., Lihavainen, H., Nilsson, D., Facchini, M. C., Cavalli, F., Fuzzi, S., Hoffmann, T., Arnold, F., Hanke, M., Sellegri, K., Umann, B., Junkermann, W., Coe, H., Allan, J. D., Alfarra, M. R., Worsnop, D. R., Riekkola, M. -L., Hytylinen, T., and Viisanen, Y.: The role of VOC oxidation products in continental new particle formation, Atmos. Chem. Phys., 8, 2657–2665, doi:10.5194/acp-8-2657-2008, 2008.

Loveland, T. R. and Belward, A. S.: The International Geosphere Biosphere Programme Data and Information System global land cover data set (DISCover), Acta Astronaut., 41, 681–689, 1997.

Martensson, E. M., Nilsson, E. D., de Leeuw, G., Cohen, L. H., and Hansson, H. C.: Laboratory simulations and parameterization of the primary marine aerosol production, J. Geophys. Res.-Atmos., 108, 4297, doi:10.1029/2002JD002263, 2003.

Merikanto, J., Spracklen, D. V., Mann, G. W., Pickering, S. J., and Carslaw, K. S.: Impact of nucleation on global CCN, Atmos. Chem. Phys., 9, 8601–8616, doi:10.5194/acp-9-8601-2009, 2009.

Petäj"a, T., Mauldin, III, R. L., Kosciuch, E., McGrath, J., Nieminen, T., Paasonen, P., Boy, M., Adamov, A., Kotiaho, T., and Kulmala, M.: Sulfuric acid and OH concentrations in a boreal forest site, Atmos. Chem. Phys., 9, 7435–7448, doi:10.5194/acp-9-7435-2009, 2009.

Real, E., Law, K. S., Weinzierl, B., Fiebig, M., Petzold, A., Wild, O., Methven, J., Arnold, S., Stohl, A., Huntrieser, H., Roiger, A., Schlager, H., Stewart, D., Avery, M., Sachse, G., Browell, E., Ferrare, R., and Blake, D.: Processes influencing ozone levels in Alaskan forest fire plumes during long-range transport over the North Atlantic, J. Geophys. Res.-Atmos., 112, D10S41, doi:10.1029/2006JD007576, 2007.

Riipinen, I., Sihto, S.-L., Kulmala, M., Arnold, F., Dal Maso, M., Birmili, W., Saarnio, K., Teinil, K., Kerminen, V.-M., Laaksonen, A., and Lehtinen, K. E. J.: Connections between atmospheric sulphuric acid and new particle formation during QUEST IIIIV campaigns in Heidelberg and Hyytiälä, Atmos. Chem. Phys., 7, 1899–1914, doi:10.5194/acp-7-1899-2007, 2007.

Simpson, D., Guenther, A., Hewitt, C. N., and Steinbrecher, R.: Biogenic emissions in europe .1. estimates and uncertainties, J. Geophys. Res.-Atmos., 100, 22875–22890, 1995.

Spracklen, D. V., Carslaw, K. S., Kulmala, M., Kerminen, V.-M., Mann, G. W., and Sihto, S.-L.: The contribution of boundary layer nucleation events to total particle concentrations on regional and global scales, Atmos. Chem. Phys., 6, 5631–5648, doi:10.5194/acp-6-5631-2006, 2006.

Tarvainen, V., Hakola, H., Rinne, J., Hellen, H., and Haapanala, S.: Towards a comprehensive emission inventory of terpenoids from boreal ecosystems, Tellus B, 59, 526–534, 2007.

Tunved, P., Hansson, H. C., Kerminen, V. M., Strom, J., Dal Maso, M., Lihavainen, H., Viisanen, Y., Aalto, P. P., Komppula, M., and Kulmala, M., High natural aerosol loading over boreal forests, Science, 312, 261–263, 2006a.

Tunved, P., Hansson, H.-C., Kulmala, M., Aalto, P., Viisanen, Y., Karlsson, H., Kristensson, A., Swietlicki, E., Dal Maso, M., Strm, J., and Komppula, M.: One year boundary layer aerosol size distribution data from five nordic background stations, Atmos. Chem. Phys., 3, 2183–2205, doi:10.5194/acp-3-2183-2003, 2003.

Tunved, P., Korhonen, H., Strom, J., Hansson, H. C., Lehtinen, K. E. J., and Kulmala, M.: Is nucleation capable of explaining observed aerosol integral number increase during southerly transport over Scandinavia ? Tellus B, 58, 129–140, 2006b.

Tunved, P., Nilsson, E. D., Hansson, H. C., Strom, J., Kulmala, M., Aalto, P., and Viisanen, Y.: Aerosol characteristics of air masses in northern Europe: Influences of location, transport, sinks, and sources, J. Geophys. Res.-Atmos., 110, D07201, doi:10.1029/2004JD005085, 2005.